

---

# Conformal Frequency Estimation with Sketched Data

---

**Matteo Sesia**

Department of Data Sciences and Operations  
University of Southern California  
Los Angeles, California, USA  
sesia@marshall.usc.edu

**Stefano Favaro**

Department of Economics and Statistics  
University of Torino and Collegio Carlo Alberto  
Torino, Italy  
stefano.favaro@unito.it

## Abstract

A flexible conformal inference method is developed to construct confidence intervals for the frequencies of queried objects in very large data sets, based on a much smaller sketch of those data. The approach is data-adaptive and requires no knowledge of the data distribution or of the details of the sketching algorithm; instead, it constructs provably valid frequentist confidence intervals under the sole assumption of data exchangeability. Although our solution is broadly applicable, this paper focuses on applications involving the count-min sketch algorithm and a non-linear variation thereof. The performance is compared to that of frequentist and Bayesian alternatives through simulations and experiments with data sets of SARS-CoV-2 DNA sequences and classic English literature.

## 1 Introduction

### 1.1 Frequency queries from sketched data

An important task in computer science is to estimate the frequency of an object given a lossy compressed representation, or *sketch*, of a big data set [1, 2]; this task has real-world relevance in diverse fields including machine learning [3], cybersecurity [4], natural language processing [5], genetics [6], and privacy [7]. Practically, sketching may be motivated for example by memory limitations, as large numbers of distinct symbols may otherwise be computationally expensive to analyze [6], or by privacy constraints, in situations where the original data contain sensitive information [8]. There exist many sketching algorithms, several of which are specifically designed to enable efficient approximations of the empirical frequencies of the compressed objects. We refer to the monograph of [9] for a recent review of sketching. Building upon this literature, our paper studies the problem of precisely quantifying the uncertainty of empirical frequency estimates obtained from sketched data without making strong assumptions about the inner workings of the sketching procedure, which may be complex and even unknown. The key ideas of the described solution are in principle applicable regardless of how the data are compressed, but the exposition of this paper will focus for simplicity on a particularly well-known sketching algorithm and some widely applied variations thereof.

### 1.2 The count-min sketch

The count-min sketch (CMS) of [10] is a renowned algorithm for compressing a data set of  $m$  objects  $Z_1, \dots, Z_m \in \mathcal{Z}$ , with  $\mathcal{Z}$  being a discrete (and possibly infinite) space, into a representation with reduced memory footprint, while allowing simple approximate queries about the observed frequency of any possible  $z \in \mathcal{Z}$ . At the heart of the CMS lie  $d \geq 1$  different  $w$ -wide *hash* functions  $h_j : \mathcal{Z} \rightarrow [w] := \{1, \dots, w\}$ , for all  $j \in [d] := \{1, \dots, d\}$  and some integer  $w \geq 1$ . Each hash function maps the elements of  $\mathcal{Z}$  into one of  $w$  possible buckets, and it is designed to ensure that distinct values of  $z$  populate the buckets uniformly. Hash functions are typically chosen at random from a *pairwise independent* family  $\mathcal{H}$ , which ensures the probability (over the randomness in the

choice of hash functions) that two distinct objects  $z_1, z_2 \in \mathcal{Z}$  are mapped by two different hash functions into the same bucket is equal to  $1/w^2$ . The data set  $Z_1, \dots, Z_m$  is then compressed into a sketch matrix  $C \in \mathbb{N}^{d \times w}$  with row sums equal to  $m$ . The element in the  $j$ -th row and  $k$ -th column of  $C$  counts the number of data points mapped by the  $j$ -th hash function into the  $k$ -th bucket:

$$C_{j,k} = \sum_{i=1}^m \mathbb{1}[h_j(Z_i) = k], \quad j \in [d]. \quad (1)$$

Because  $d$  and  $w$  are such that  $d \cdot w \ll m$ , the matrix  $C$  loses information compared to the full data set, but it has the advantage of requiring much less space to store.

Given a sketch  $C$  from (1), one may want to answer queries about the original data. A fundamental instance of this problem consists in estimating the true empirical frequency of an object  $z \in \mathcal{Z}$ :

$$f_m(z) := \sum_{i=1}^m \mathbb{1}[Z_i = z]. \quad (2)$$

One solution is to return the smallest count among the  $d$  buckets into which  $z$  is mapped:

$$\hat{f}_{\text{up}}^{\text{CMS}}(z) = \min_{j \in [d]} \{C_{j, h_j(z)}\} \geq f_m(z). \quad (3)$$

This procedure is outlined in Algorithm A1 (Appendix A1) and it provides a deterministic upper bound for  $f_m(z)$  [10]. Of course,  $\hat{f}_{\text{up}}^{\text{CMS}}(z)$  tends to overestimate  $f_m(z)$  due to possible hash collisions. But the independence of the hash functions ensures collisions are not too common, leading to a classical probabilistic lower bound for  $f_m(z)$ .

**Theorem 1** ([10]). *Fix any  $\delta, \epsilon \in (0, 1)$ . Suppose  $d = \lceil -\log \delta \rceil$  and  $w = \lceil e/\epsilon \rceil$ . Then,  $\mathbb{P}_{\mathcal{H}}[f_m(z) \geq \hat{f}_{\text{up}}^{\text{CMS}}(z) - \epsilon m] \geq 1 - \delta$  for any fixed  $z \in \mathcal{Z}$ , where  $\hat{f}_{\text{up}}^{\text{CMS}}(z)$  is as in (1) and depends on  $d, w$ .*

For example, if  $d = 3$ , this says that a 95% lower bound on  $f_m(z)$  is  $\hat{f}_{\text{up}}^{\text{CMS}}(z) - \lceil e \cdot m/w \rceil$ . The subscript  $\mathcal{H}$  in Theorem 1 clarifies that the randomness is with respect to the hash functions, while  $Z_1, \dots, Z_m$  and  $z$  are fixed. The above bound can be useful to inform the choices of  $d$  and  $w$  prior to sketching, but it is not fully satisfactory as a way of quantifying the uncertainty about the true frequency of a given query. First, it is often too conservative [11] if the data are randomly sampled from some distribution as opposed to being fixed. Second, it is not flexible:  $\delta$  cannot be chosen by the user because it is fixed by  $d$ , and  $\epsilon$  is uniquely determined by the hash width. Thus, in general Theorem 1 cannot give a reasonably tight confidence interval for  $f_m(z)$  at an arbitrary level. As we will discuss below, these limitations can be overcome by assuming the data are sampled randomly.

### 1.3 Uncertainty estimation for sketching with random data

An alternative approach to computing probabilistic lower and upper bounds for  $f_m(z)$  was proposed by [11] in order to address the often excessive conservativeness of the classical bounds described above. The approach of [11] is based on bootstrapping ideas and departs from classical analysis of the CMS as it leverages randomness in the data instead of randomness in the hash functions. Precisely, [11] assumes the data and the queried object are independent and identically distributed (i.i.d.) random samples from some unknown distribution. These assumptions may not always be justified in practice, but they are useful because they can lead to much more informative confidence intervals. In fact, the confidence intervals described by [11] are nearly exact and optimal for the CMS, up to a possible finite-sample discrepancy between the bootstrap and population distributions.

A limitation of the bootstrap method of [11] is that it relies on the specific *linear* structure of the CMS—the sketch matrix  $C$  in (3) can be written as a linear combination of the true frequencies of all objects in the data set—and thus the idea is not easily extendable to other sketching algorithms that may perform better than the CMS in practice. One issue with the CMS is that it is relatively sensitive to random hash collisions, which can result in overly conservative deterministic upper bounds. This challenge has motivated the development of alternative *non-linear* sketching algorithms, such as the CMS with *conservative updates* (CMS-CU). Whenever a new object  $Z_i$  is sketched, the CMS-CU only updates the row of  $C$  with the smallest value of  $C_{j, h_j(z)}$ , leaving the other counters unaltered. Then, the same CMS deterministic upper bound in (3) remains valid. This procedure is outlined in Algorithm A2. This non-linear approach can lead to much higher query accuracy compared to the vanilla CMS [12], but the theoretical analysis of the CMS-CU beyond a deterministic upper bound is more challenging, and it appears to be a relatively less explored topic.

## 1.4 Contributions

This paper develops a novel method for constructing valid and reasonably tight frequentist confidence intervals for frequency queries based on sketched data. Our method works seamlessly with the CMS-CU as well as with any possibly unknown sketching algorithm. The solution assumes the data and the query are random samples from some unknown population, making only minimal exchangeability assumptions about this data generating process. Although our method requires higher computational power and memory usage compared to pure sketching, the additional cost of our uncertainty estimates will be negligible compared to the typical size of the data sets involved.

## 1.5 Related work

Different types of lower bounds have been developed for the CMS [9], although most treat the data as fixed and only utilize the hashing randomness, similarly to Theorem 1. More recently, uncertainty estimation for the CMS based on data randomness has been studied by [11] from a frequentist perspective, as mentioned in Section 1.3, and by [13, 14] from a Bayesian perspective. More precisely, [13] and [14] model the data with a prior distribution and compute the posterior of the queried frequencies given the sketch. Our work is closer to [11] in that we treat the data as random while seeking frequentist probabilistic guarantees. However, our approach is very different from that of [11]: the latter exploits the specific linear structure of the CMS, while we view the sketch as a black box and utilize conformal inference to obtain exact finite-sample inferences.

Conformal inference was pioneered by Vovk and collaborators [15] and brought to the statistics spotlight by [16]. Although primarily conceived for supervised prediction [17–21], conformal inference has found many other applications including outlier detection [22], causal inference [23], and survival analysis [24]. To the best of our knowledge, its potential for sketching remained untapped until now. There exist many algorithms for using sketches to compute approximate frequency queries; some are similar to the CMS [9, 25–27], while others are more complicated and may involve complex learning algorithms [28, 29]. In theory our method is applicable to all of them, but here we focus more on the CMS and variations thereof because it is a classic algorithm and it provides a familiar example that facilitates the exposition. As we will make use of conformal inference, a brief review of the relevant technical background is provided in the next section.

## 2 Preliminaries on conformal prediction

Conformal prediction is typically concerned with *supervised learning*, in which the data samples are pairs  $(X_i, Y_i)$ , with  $X_i$  indicating a vector of *features* for the  $i$ -th observation and  $Y_i$  denoting the corresponding continuous (or discrete) *label*. In supervised learning, the goal is to use the information contained in  $(X_1, Y_1), \dots, (X_m, Y_m)$  to learn a mapping between features and labels that can allow one to predict as accurately as possible the unseen label  $Y_{m+1}$  of a new sample with features  $X_{m+1}$ . In particular, conformal prediction assumes that  $(X_1, Y_1), \dots, (X_{m+1}, Y_{m+1})$  are exchangeable random samples from some unknown joint distribution over  $(X, Y)$  and then constructs a prediction interval  $[\hat{L}_{m,\alpha}(X_{m+1}), \hat{U}_{m,\alpha}(X_{m+1})]$  with guaranteed *marginal coverage*:

$$\mathbb{P}[\hat{L}_{m,\alpha}(X_{m+1}) \leq Y_{m+1} \leq \hat{U}_{m,\alpha}(X_{m+1})] \geq 1 - \alpha, \quad (4)$$

for any fixed  $\alpha \in (0, 1)$ . Conformal prediction is flexible, as it can leverage any machine learning algorithm to approximately reconstruct the relation between  $X$  and  $Y$ , thus yielding relatively short intervals satisfying (4). Note that, while it is appropriate to focus on conformal intervals in this paper, similar techniques can also be utilized to construct more general prediction sets [30, 31].

The simplest version of conformal prediction begins by randomly splitting the available observations into two disjoint subsets, assumed for simplicity to have equal size  $n = m/2$ . The first  $n$  samples are spent to fit a black-box machine learning model for predicting  $Y$  given  $X$ ; e.g., a neural network or a random forest. The out-of-sample predictive accuracy of this model is then measured in terms of a *conformity score* for each of the  $n$  hold-out data points. In combination with the model learnt from the first half of the data, the empirical distribution of these scores is translated into a recipe for constructing prediction intervals for future test points as a function of  $X_{m+1}$ ; these intervals are guaranteed to cover  $Y_{n+1}$  with probability at least  $1 - \alpha$ , treating all data as random. The details of this procedure will be clarified shortly. Importantly, the coverage holds exactly in finite samples,

regardless of the accuracy of the machine learning model, as long as  $X_{m+1}$  is exchangeable with the  $n$  hold-out data points. Note that it is unnecessary for the training data to be also exchangeable, as these may be seen as fixed, but it is sometimes easier to say all data points are exchangeable.

The implementation of conformal inference depends on the choice of conformity scores. While several different options exist, an intuitive and general explanation is the following. Imagine that associated with the fitted machine learning model there exists a *nested sequence* [32] of prediction intervals  $[\hat{L}_{m,\alpha}(x; t), \hat{U}_{m,\alpha}(x; t)]$  for each possible  $x$ . This sequence is indexed by  $t \in \mathcal{T} \subseteq \mathbb{R}$ , which may be either discrete or continuous, and it is increasing:  $\hat{L}_{m,\alpha}(x; t_2) \leq \hat{L}_{m,\alpha}(x; t_1)$  and  $\hat{U}_{m,\alpha}(x; t_2) \geq \hat{U}_{m,\alpha}(x; t_1)$  for all  $t_2 \geq t_1$ . Further, assume there exists  $t_\infty \in \mathcal{T}$  such that  $\hat{L}_{m,\alpha}(x; t_\infty) \leq Y \leq \hat{U}_{m,\alpha}(x; t_\infty)$  almost surely for all  $x$ . For example, one may consider a sequence  $\hat{\psi}_m(x) \pm t$ , where  $\hat{\psi}_m$  is a regression function for a bounded label  $Y$  given  $X$  learnt by the black-box machine learning model and  $t$  plays the role of a predictive standard error. Then, the conformity score for a data point with features  $X = x$  and label  $Y = y$  can be defined as the smallest index  $t$  such that  $y$  is contained in the sequence of prediction intervals corresponding to  $x$ :

$$E(X, Y) := \min \{t \in \mathcal{T} : Y \in [\hat{L}_{m,\alpha}(x; t), \hat{U}_{m,\alpha}(x; t)]\}. \quad (5)$$

The conformal prediction rule is then easily stated. Let  $\mathcal{I}^{\text{calib}} \subset \{1, \dots, m\}$  be the subset of hold-out data points, assumed without loss of generality to have size  $n = m/2$ . Let  $\hat{Q}_{n,1-\alpha}$  be the  $\lceil (1-\alpha)(n+1) \rceil$  smallest value among the  $n$  conformity scores  $E(X_i, Y_i)$  evaluated for all  $i \in \mathcal{I}^{\text{calib}}$ . The conformal prediction interval for a new data point with features  $X_{m+1}$  is:

$$[\hat{L}_{m,\alpha}(X_{m+1}; \hat{Q}_{n,1-\alpha}), \hat{U}_{m,\alpha}(X_{m+1}; \hat{Q}_{n,1-\alpha})]. \quad (6)$$

Intuitively, this satisfies (4) because  $Y_{m+1}$  is outside (6) if and only if  $E(X_{m+1}, Y_{m+1}) > \hat{Q}_{n,1-\alpha}$ . The rest of the proof is a simple exchangeability argument; see [20] or the proof of Theorem 2.

### 3 Conformalized sketching

#### 3.1 Exchangeable queries and marginal coverage

Assume the  $m$  data points to be sketched,  $Z_1, \dots, Z_m \in \mathcal{Z}$ , are exchangeable random samples (a weaker condition than i.i.d.) from some distribution  $P_{\mathcal{Z}}$  on  $\mathcal{Z}$ . Although  $P_{\mathcal{Z}}$  may be arbitrary and unknown, our framework is more restrictive compared to the classical setting reviewed in Section 1.2, which treats the data as fixed and thus can also handle non-stationary streams or adversarial cases. Yet, imagining the data as approximately i.i.d. samples from some distribution is not an unprecedented idea in the context of sketching [11, 13, 14], and it may be justified when objects from a large data set are processed in a random order; see Sections 4 and 5. As we shall see below, data exchangeability can be an extremely useful assumption because it allows one to obtain powerful inferences while taking a completely agnostic view of the inner workings of the sketching algorithm.

Consider an arbitrary *sketching* function  $\phi : [\mathcal{Z}]^m \rightarrow \mathcal{C}$ , where  $\mathcal{C}$  is a space with lower dimensions compared to  $[\mathcal{Z}]^m$ . For example,  $\phi$  may represent the sketching performed by the CMS or CMS-CU, in which case  $\mathcal{C} = \mathbb{N}^{d \times w}$ , for some  $d, w$  such that  $d \cdot w \ll m$ . In general, we will treat  $\phi$  as a *black box* and allow it to be anything, possibly involving random hashing or any other data compression technique. The goal is to leverage the data exchangeability and the information in  $\phi(Z_1, \dots, Z_m)$  to estimate the unobserved true empirical frequency  $f_m(z)$  of some object  $z \in \mathcal{Z}$ , defined as in (2), while accounting for uncertainty. More precisely, although still informally speaking, we would like to construct a *confidence interval*  $[\hat{L}_{m,\alpha}(z), \hat{U}_{m,\alpha}(z)]$  guaranteed to contain  $f_m(z)$  “with probability at least  $1 - \alpha$ ”, where the randomness here is with respect to the random data sampling.

One way to address the above problem is to imagine the query  $z$  is also randomly sampled exchangeably with  $Z_1, \dots, Z_m$ . This is a convenient but quite strong assumption that will be partly relaxed later. With this premise, we refer to  $z$  as  $Z_{m+1}$  and focus on computing a confidence interval  $[\hat{L}_{m,\alpha}(Z_{m+1}), \hat{U}_{m,\alpha}(Z_{m+1})]$  depending on  $\phi(Z_1, \dots, Z_m)$  that is reasonably short and guarantees marginal coverage of the true unknown frequency:

$$\mathbb{P}[\hat{L}_{m,\alpha}(Z_{m+1}) \leq f_m(Z_{m+1}) \leq \hat{U}_{m,\alpha}(Z_{m+1})] \geq 1 - \alpha, \quad (7)$$

where the probability is with respect to the data in  $Z_1, \dots, Z_m$  as well as to the randomness in the query  $Z_{m+1}$ . The interpretation of (7) is as follows: the interval will cover the true frequency  $f_m(Z)$  for at least a fraction  $1 - \alpha$  of all future test points  $Z$  on average, if the queries and the sketched data are re-sampled exchangeably. In Section 3.3, we will develop a method for constructing reasonably tight confidence intervals satisfying (7) exactly. This is already a non-trivial result on its own, but marginal coverage is not fully satisfactory because some objects may be queried more often than others, and therefore not all of our *distinct* inferences are equally reliable. In particular, the confidence intervals for rare queries may have lower coverage, as illustrated by the following thought experiment. Imagine  $P_Z$  has support on  $\mathcal{Z} = \{0, 1, 2, \dots, 10^{100}\}$ , with  $\mathbb{P}[Z_i = 0] = 0.95$  and  $\mathbb{P}[Z_i = z] = 0.05/(|\mathcal{Z}| - 1)$  for all  $z \in \mathcal{Z} \setminus \{0\}$  and  $i \geq 1$ . Then, a 95% confidence interval satisfying (7) may be completely unreliable for all but one specific query about  $f_m(0)$ .

### 3.2 Beyond full exchangeability with approximate frequency-conditional coverage

To begin addressing the limitations of marginal coverage, Section 3.3 will develop a more refined method for constructing confidence intervals that are simultaneously valid for both rare and common random queries. Our approach re-purposes relevant ideas from Mondrian conformal inference [33], which have been utilized before to construct prediction sets with label-conditional coverage for classification problems [15, 30, 34]. However, departing from the typical approach in classification, we will not seek perfect coverage conditional on the exact true frequency of the queried object. In fact, that problem would be impossible to solve without stronger assumptions [35], because  $f_m(Z_{m+1})$  can take a very large number of possible values when the sketched data set is big. Instead, we will focus on achieving a relaxed concept of frequency-conditional coverage which groups together different queries of objects that appear a similar number of times within the sketched data set. Precisely, let us fix any partition  $\mathcal{B} = (B_1, \dots, B_L)$  of  $\{1, \dots, m\}$  into  $L$  bins such that each  $B_l$  is a sub-interval of  $\{1, \dots, m\}$ , for some relatively small integer  $L$ . In theory, this partition should be fixed prior to seeing the data and may not depend on the new query  $Z_{m+1}$ . Our goal is to construct a confidence interval  $[\hat{L}_{m,\alpha}(Z_{m+1}), \hat{U}_{m,\alpha}(Z_{m+1})]$  depending on  $\phi(Z_1, \dots, Z_m)$  and  $\mathcal{B}$  that is reasonably short and satisfies the following notion of *frequency-range conditional coverage*:

$$\mathbb{P}[\hat{L}_{m,\alpha}(Z_{m+1}) \leq f_m(Z_{m+1}) \leq \hat{U}_{m,\alpha}(Z_{m+1}) \mid f_m(Z_{m+1}) \in B] \geq 1 - \alpha, \quad \forall B \in \mathcal{B}. \quad (8)$$

The choice of  $\mathcal{B}$  involves some trade-offs: finer partitions (larger  $L$ ) yield more reliable theoretical guarantees but possibly wider confidence intervals; in particular, intervals associated with a bin  $B$  may tend to be wider if  $\mathbb{P}[Z \in B]$  is small. In practice, we will adopt  $|\mathcal{B}| = 5$  later in this paper, but much larger  $|\mathcal{B}|$  can be utilized when working with very big data, as it will become clear below.

### 3.3 Conformalization methodology

In the attempt of adapting conformal inference to address our sketching problem, the first difficulty is that the latter is a data recovery problem, not a supervised prediction task. We propose to overcome this challenge by storing in memory the true frequencies for all objects in the first  $m_0$  observations, with  $m_0 \ll m$  but sufficiently large subject to memory constraints. Without loss of generality, assume  $m_0 \ll m$ ; otherwise, the problem becomes trivially easy. Let  $n \leq m_0$  indicate the number of distinct objects among the first  $m_0$  observations. The memory required to store these frequencies is  $O(n)$ , which will typically be negligible as long as  $m_0$  is also small compared to the size of the sketch,  $|\mathcal{C}|$ . This approach turns our problem into a supervised prediction one, as detailed below.

During an initial *warm-up* phase, the frequencies of the  $n$  distinct objects among the first  $m_0$  observations from the data stream,  $Z_1, \dots, Z_{m_0}$ , are stored exactly into:

$$f_{m_0}^{\text{wu}}(z) := \sum_{i=0}^{m_0} \mathbb{1}[Z_i = z]. \quad (9)$$

Next, the remaining  $m - m_0$  data points are streamed and sketched, storing also the true frequencies for all instances of objects already seen during the warm-up phase. In other words, the following counters are computed and stored along with the sketch  $\phi(Z_{m_0+1}, \dots, Z_m)$ :

$$f_{m-m_0}^{\text{sv}}(z) := \begin{cases} \sum_{i=m_0+1}^m \mathbb{1}[Z_i = z], & \text{if } f_{m_0}^{\text{wu}}(z) > 0, \\ 0, & \text{otherwise.} \end{cases} \quad (10)$$

Again, this requires only  $O(n)$  memory. Now, let us define the variable  $Y_i$  for all  $i \in \{1, \dots, m_0\} \cup \{m+1\}$  as the true frequency of  $Z_i$  among  $Z_{m_0+1}, \dots, Z_m$ :

$$Y_i := \sum_{i'=m_0+1}^m \mathbb{1}[Z_{i'} = Z_i]. \quad (11)$$

Note that  $Y_i$  is observable for  $i \in \{1, \dots, m_0\}$ , in which case  $Y_i = f_{m-m_0}^{\text{sv}}(Z_i)$ . For a new query,  $Z_{m+1}$  is the target of inference—in truth, the target is  $f_m(Z_i) = Y_i + f_{m_0}^{\text{wu}}(Z_i)$ , but the second term is already known exactly. To complete the connection between sketching and supervised conformal prediction, one still needs to define meaningful features  $X$ , and this is where the sketch  $\phi(Z_{m_0+1}, \dots, Z_m)$  comes into play. For each  $i \in \{1, \dots, m_0\} \cup \{m+1, \dots\}$ , define  $X_i$  as the vector containing the object of the query as well as all the information in the sketch:

$$X_i := (Z_i, \phi(Z_{m_0+1}, \dots, Z_m)). \quad (12)$$

The following result establishes that the pairs  $(X_1, Y_1), \dots, (X_{m_0}, Y_{m_0}), (X_{m+1}, Y_{m+1})$  are exchangeable with one another. This anticipates that conformal prediction techniques can be applied to the supervised observations  $(X_1, Y_1), \dots, (X_{m_0}, Y_{m_0})$  to predict  $Y_{m+1}$  given  $X_{m+1}$ , guaranteeing the marginal coverage property in (7). All mathematical proofs are in Appendix A2.

**Proposition 1.** *If the data  $Z_1, \dots, Z_{m+1}$  are exchangeable, then the pairs of random variables  $(X_1, Y_1), \dots, (X_{m_0}, Y_{m_0}), (X_{m+1}, Y_{m+1})$  defined in (11)–(12) are exchangeable with one another.*

Confidence intervals satisfying frequency-range coverage (8) can be obtained by modifying the standard conformal inference procedure as outlined in Algorithm A3, whose details are deferred to Appendix A1 for lack of space. First, each point  $(X_i, Y_i)$  in  $\mathcal{I}^{\text{calib}} = \{1, \dots, m_0\}$  is assigned to the appropriate frequency bin based on  $Y_i$ . Define  $n_l$  as the number of calibration points in bin  $B_l$ , for all  $l \in \{1, \dots, L\}$ . Then,  $\hat{Q}_{n_l, 1-\alpha}(B_l)$  is defined as the  $\lceil (1-\alpha)(n_l+1) \rceil$  smallest value among the  $n_l$  scores assigned to bin  $B_l$ . Finally, the confidence interval for a new random query  $X_{m+1}$  is:

$$[\hat{L}_{m,\alpha}(X_{m+1}; \hat{Q}_{n, 1-\alpha}^*), \hat{U}_{m,\alpha}(X_{m+1}; \hat{Q}_{n, 1-\alpha}^*)],$$

where

$$\hat{Q}_{n, 1-\alpha}^* := \max_{l \in \{1, \dots, L\}} \hat{Q}_{n_l, 1-\alpha}(B_l),$$

and  $[\hat{L}_{m,\alpha}(\cdot; t), \hat{U}_{m,\alpha}(\cdot; t)]$  is a rule for computing a nested sequence of intervals depending on  $Z_{m+1}$  and  $\phi(Z_{m_0+1}, \dots, Z_m)$ , assumed by convention to be increasing in  $t$ . Examples of such rules are in the next section. Importantly, these rules may involve parameters to be fitted on a subset of  $m_0^{\text{train}}$  supervised data points  $(X_i, Y_i)$  for  $i \in \{1, \dots, m_0^{\text{train}}\}$ , as long as the scores are only evaluated on the remaining  $m_0 - m_0^{\text{train}}$  points. The following result states that the confidence interval output by Algorithm A3 has the desired frequency-range conditional coverage.

**Theorem 2.** *If the data  $Z_1, \dots, Z_{m+1}$  are exchangeable, the confidence interval output by Algorithm A3 satisfies the frequency-range conditional coverage property defined in (8).*

Theorem 2 also implies that confidence intervals satisfying the weaker marginal coverage property defined in (7) can be obtained by applying Algorithm A3 with the trivial partition  $\mathcal{B}$  dividing the range of possible frequencies into a single bin of size  $m$ , because (7) is a special case of (8). Note also that Algorithm A3 could be trivially modified to output perfect “singleton” confidence intervals for any new queries that happen to be identical to an object previously observed during the warm-up phase. We will not take advantage of this fact in the experiments presented in this paper to provide a fairer comparison with alternative methods which do not involve a similar warm-up phase.

### 3.4 Conformity scores for one-sided confidence intervals

Algorithm A3 can accommodate virtually any data-adaptive rule for computing nested confidence intervals, which may depend on  $Z_{m+1}$  and on the sketch  $\phi := \phi(Z_{m_0+1}, \dots, Z_m)$ . Two concrete options are presented here. For simplicity, we focus on one-sided confidence intervals; that is, we seek a  $1 - \alpha$  lower bound for  $f_m(X_{m+1})$ . This is useful when a deterministic upper bound  $\hat{f}_{\text{up}}(Z_{m+1}) \geq f_m(Z_{m+1})$  is already available, as it is the case with the CMS or CMS-CU. Then,

one can simply set  $\hat{U}_{m,\alpha}((z, \phi); t) := \hat{f}_{\text{up}}(z)$  and focus on computing  $\hat{L}_{m,\alpha}(\cdot; t)$ . The construction of two-sided confidence intervals is explained in Appendix A1.4 due to lack of space.

To construct the lower bound  $\hat{L}_{m,\alpha}(\cdot; t)$  of a one-sided interval, the first option is to use a fixed rule:

$$\hat{L}_{m,\alpha}^{\text{fixed}}((z, \phi); t) := \max\{0, \hat{f}_{\text{up}}(Z_{m+1}) - t\}, \quad t \in \{0, 1, \dots, m\}. \quad (13)$$

In words, the lower bound for  $f_m(Z_{m+1})$  in (14) is defined by shifting the deterministic upper bound downward by a constant  $t$ . The appropriate value of  $t$  guaranteeing the desired coverage for future random queries is calibrated by Algorithm A3. This approach is intuitive, and it is very similar to the optimal solution of [11] for the special case of the CMS. Further, it does not need training data, so all  $m_0$  observations with tracked frequencies can be utilized for computing conformity scores.

The second option involves training but has the advantage of being more flexible; this is inspired by the methods of [36, 37] for regression. Concretely, consider a machine learning model that takes as input the known upper bound  $\hat{f}_{\text{up}}(Z_i)$  and estimates the conditional distribution of  $\hat{f}_{\text{up}}(Z_i) - f_m(Z_i)$  given  $\hat{f}_{\text{up}}(Z_i)$ . For example, think of a multiple quantile neural network [38] or a quantile random forest [39]. After fitting this model on the  $m_0^{\text{train}}$  supervised data points  $(X_i, Y_i)$  allocated for training, let  $\hat{q}_t$  be the estimated  $\alpha_t$  lower quantile of the of  $\hat{f}_{\text{up}}(Z_i) - f_m(Z_i) \mid \hat{f}_{\text{up}}(Z_i)$ , for all  $t \in [1, \dots, T]$  and some fixed sequence  $1 = \alpha_1 < \dots < \alpha_T = 0$ . Without loss of generality, assume the machine learning model is that  $\hat{q}_0 = 0$  and  $\hat{q}_T = m$ . Then, define  $\hat{L}_{m,\alpha}(\circ; t)$  as:

$$\hat{L}_{m,\alpha}^{\text{adaptive}}((z, \phi); t) := \max\left\{0, \hat{f}_{\text{up}}(X_{m+1}) - \hat{q}_t\left(\hat{f}_{\text{up}}(X_{m+1})\right)\right\}, \quad t \in \{0, 1, \dots, m\}. \quad (14)$$

This second approach can lead to a lower bound whose distance from the upper bound is adaptive. This is an advantage because some sketching algorithms may introduce higher uncertainty about common queries compared to rarer ones, or vice versa, and such patterns can be learnt given sufficient data. Of course, the two above examples of  $\hat{L}_{m,\alpha}(\cdot; t)$  are not exhaustive. Algorithm A3 can be applied in combination with any rule for computing nested sequences of lower bounds, and it can leverage all high-dimensional information contained in  $\phi(Z_{m_0+1}, \dots, Z_m)$ , not just the deterministic upper bound for the CMS and CMS-CU. However, the applications in this paper focus on the CMS and CMS-CU, so other families of lower bounds are not discussed here.

## 4 Applications

### 4.1 Experiments with synthetic data sets

Conformalized sketching is applied with the two types of conformity scores described in Section 3.4, focusing on the construction of one-sided confidence intervals. Additional experiments involving two-sided intervals are described in Appendix A4. The adaptive scores utilized in this section are based on an isotonic distributional regression model [40]. The goal is to compute lower frequency bounds for random queries based on simulated data compressed by the CMS-CU, implemented with  $d = 3$  hash functions of width  $w = 1000$ . In particular,  $m = 100,000$  observations are sampled i.i.d. from some distribution specified below. The first  $m_0 = 5000$  observations are stored without loss during the warm-up phase, as outlined in Algorithm A3, while the remaining 95,000 are compressed by the CMS-CU. The conformity scores are evaluated separately within  $L = 5$  frequency bins, seeking the frequency-range conditional coverage property defined in (8). The bins are determined in a data-driven fashion so that each contains approximately the same probability mass; in practice, this is achieved by partitioning the range of frequencies for the objects tracked exactly by Algorithm A3 according to the observed empirical quantiles. Lower bounds for new queries are computed for 10,000 data points also sampled i.i.d. from the same distribution. The quality of these bounds is quantified with two metrics: the mean *length* of the resulting confidence intervals and the coverage the proportion of queries for which the true frequency is correctly covered, or empirical *coverage*. The performance is averaged over 10 independent experiments.

Experiments are performed on synthetic data sampled from two families of distributions. First, we consider a Zipf distribution with  $\mathbb{P}[Z_i = z] = z^{-a}/\zeta(a)$  for all  $z \in \{1, 2, \dots\}$ , where  $\zeta$  is the Riemann Zeta function and  $a > 1$  is a control parameter affecting the power-law tail behavior. Second, synthetic data are generated from a random probability measure distributed as the Pitman-Yor prior [41] with a standard Gaussian base distribution and parameters  $\lambda > 0$  and  $\sigma \in [0, 1)$ , as

explained in Appendix A1.5. The parameter  $\lambda$  is set to  $\lambda = 5000$ , while  $\sigma$  is varied. For  $\sigma = 0$  the Pitman-Yor prior reduces to the Dirichlet prior [42], while  $\sigma > 0$  results in heavier tails.

Three benchmark methods are considered. The first one is the *classical* 95% lower bound in Theorem 1. The second one is the *Bayesian* method of [13], which assumes a non-parametric Dirichlet process prior for the distribution of the data stream, estimates its scaling parameter by maximizing the marginal likelihood of the observed sketch, and then computes the posterior of the queried frequencies conditional on the observed sketch. The performance of the lower 5% posterior quantile is compared to the lower bounds obtained with the other methods according to the frequentist metrics defined above. The third benchmark is the bootstrap method of [11], which is nearly exact and optimal for the vanilla CMS (up to some possible finite-sample discrepancy between the bootstrap and population distributions) but is not theoretically valid for other sketching techniques.

Figure 1 compares the performance of the conformal method to those of the three benchmarks on the Zipf data. All methods achieve marginal coverage (4), with the exception of the Bayesian approach which in this case is based on a misspecified prior. The length of the confidence intervals indicates the classical bound is very conservative, while the bootstrap and conformal methods provide relative informative bounds, particularly when  $a$  is larger and hash collisions become rarer. The conformal intervals can be the shortest ones, especially if implemented with the adaptive conformity scores. This should not be surprising because the bootstrap may not be optimal for the CMS-CU. Indeed, as shown in Figure 2, the machine learning model deployed by our adaptive scores can take advantage of the fact that this non-linear sketch allows increased precision for more common queries.

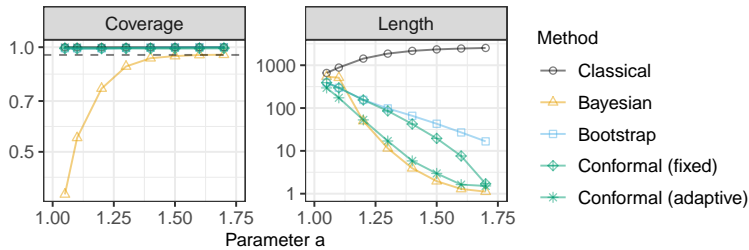


Figure 1: Coverage and length of 95% confidence intervals with data from a Zipf distribution, sketched with CMS-CU. The results are shown as a function of the Zipf tail parameter  $a$ . Standard errors would be too small to be clearly visible in this figure, and are hence omitted.

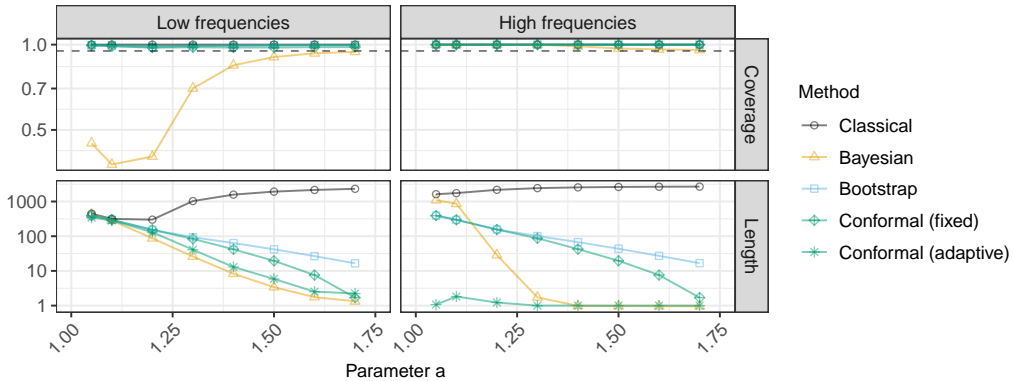


Figure 2: Performance of confidence intervals stratified by the true query frequency. Left: frequency below median; right: frequency above median. Other details are as in Figure 1.

Supplementary results reported in Appendix A3 show the CMS-CU leads to more precise queries with all methods compared to the vanilla CMS; see Figure A1. Figure A2 confirms that conformal lower bounds no longer have a clear advantage over the bootstrap ones if the data are sketched with



the vanilla CMS instead of the CMS-CU. In fact, although the conformal intervals obtained with the adaptive conformity scores can be little shorter than the bootstrap ones even for the vanilla CMS, the latter have the advantage of (approximately, in the limit of large samples) satisfying an even stronger frequency-conditional coverage property equivalent to (8) with bins of size 1 [11]. Analogous results for the experiments with Pitman-Yor process data are also in Appendix A3; see Figures A3–A6.

## 4.2 Analysis of 16-mers in SARS-CoV-2 DNA sequences

This application involves a data set of nucleotide sequences from SARS-CoV-2 viruses made publicly available by the National Center for Biotechnology Information [43]. The data include 43,196 sequences, each consisting of approximately 30,000 nucleotides. The goal is to estimate the empirical frequency of each possible *16-mer*, a distinct sequence of 16 DNA bases in contiguous nucleotides. Given that each nucleotide has one of 4 bases, there are  $4^{16} \approx 4.3$  billion possible 16-mers. Thus, exact tracking of all 16-mers is not unfeasible, which allows us to validate the sketch-based queries. Sequences containing missing values are removed during pre-processing, for simplicity.

The experiments are carried out as in Section 4.1 (processing the 16-mers in a random order to ensure their exchangeability), but a larger sample of size 1,000,000 is sketched, and the width  $w$  of the hash functions is varied. Figure 3 compares the performances of all methods as a function of the hash width, in terms of marginal coverage and mean confidence interval width. All methods achieve the desired marginal coverage, except for the Bayesian approach when  $w$  is large. For small  $w$ , all methods return intervals of similar width, because the distribution of SARS-CoV-2 16-mers frequencies is quite concentrated with relatively narrow support (Figure A7), which makes it especially difficult to compress the data without much loss. By contrast, the proposed conformal methods yield noticeably shorter confidence intervals if  $w$  is large. Figure A8 reports the same results stratified by the frequency of the queried objects, while Figure A9 confirms the advantage of sketching with the CMS-CU as opposed to the vanilla CMS. Table A1 lists 10 common and 10 rare queries along with their corresponding deterministic upper bounds for  $w = 50,000$ , comparing the lower bounds obtained with each method. Table A2 shows analogous results with  $w = 5,000$ .

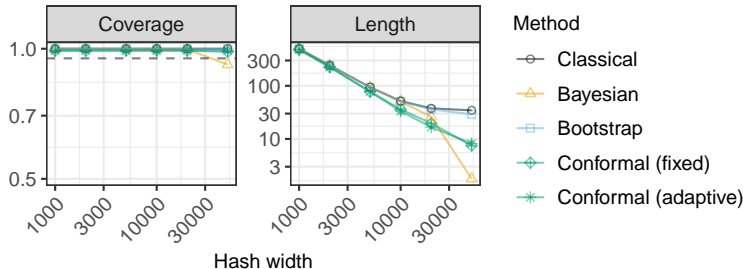


Figure 3: Performance of confidence intervals based on sketched SARS-CoV-2 sequence data. The results are shown as a function of the hash width. Other details are as in Figure 1.

Figure A10 compares the performances of different frequency *point-estimates* in terms of mean absolute deviation from the true frequency. With the classical method, we take the midpoint of the 95% confidence interval as a point estimate, although other approaches are also possible [9]. For the other methods, the point estimate is the lower confidence bound at level  $\alpha = 0.5$ ; in the Bayesian case, this is the posterior median. Although a conformal lower bound at level  $\alpha = 0.5$  is not always a reliable estimator of conditional medians [44], because the conformal coverage guarantees treat the query as random, this approach outperformed the benchmarks in all of our experiments.

## 4.3 Analysis of 2-grams in English literature

This application is based on a data set consisting of 18 open-domain classic pieces of English literature downloaded using the NLTK Python package [45] from the Gutenberg Corpus [46]. The goal is to count the frequencies of all *2-grams*—consecutive pairs of English words—across this corpus. After some basic preprocessing to remove punctuation and unusual words (only those in a dictionary of size 25,487 common English words are retained), the total number of 2-grams left in this data

set is approximately 1,700,000 (although the total number of all *possible* 2-grams within this dictionary is approximately 650,000,000). The same experiments are then carried out as in Section 4.2, sketching 1,000,000 randomly sampled 2-grams and querying 10,000 independent 2-grams. As in the previous experiments, the 2-grams are processed in a random order to ensure exchangeability.

Figure 4 shows the conformal intervals with adaptive scores achieve the desired coverage and tend to have the shortest width, while the Bayesian intervals are not valid unless the hashes are very wide. The conformal approach has a larger advantage here because these data can be compressed more efficiently compared to the one in the previous section because the frequency distribution of English 2-grams has power-law tails; see Figure A7. Additional results along the lines of those in the previous section are in Appendix A3; see Figures A11–A13 and Tables A1–A2.

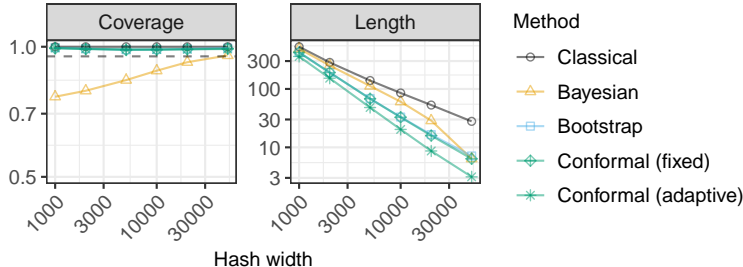


Figure 4: Performance of confidence intervals for random frequency queries, for a sketched data set of English 2-grams in classic English literature. Other details are as in Figure 3.

## 5 Discussion

Conformalized sketching is a non-parametric and data-adaptive statistical method for quantifying uncertainty in problems involving frequency estimation from sketched data. This paper has revolved around the CMS because that is a prominent technique for which several benchmarks are available. However, our method is very broadly applicable because it operates under the sole assumption of data exchangeability, without requiring any knowledge of the sketching algorithm. Of course, exchangeability is not always an appropriate assumption, and thus one may sometimes need to rely on more conservative bounds based on hashing randomness. Yet there are situations in which the sketched data can be seen as exchangeable random samples from a population. For example, in natural language processing one may wish to count the frequencies of non-contiguous tuples of words co-occurring in the same sentence within a large corpus, expanding on the example of Section 4.3. In that case, it would be unfeasible to keep track of all frequencies exactly, but our approach would be applicable as long as the tuples are sketched and queried in a random order. One limitation of conformalized sketching is that it does not provide guarantees about the expected proportion of correct *unique* queries. In fact, if the queries are randomly sampled exchangeably with the sketched data points, some of them may be redundant. Even though the expected proportion of incorrect unique queries is sometimes below  $\alpha$  (Figures A14–A15), this is not always the case (Figure A16). It may be possible to modify our procedure to achieve this additional guarantee, but we leave this problem for future work. Future research may also study theoretically, in some settings, the length of our conformal confidence intervals, following for example an approach similar to those of [16, 47].

Accompanying software and data are available online at <https://github.com/mnesia/conformalized-sketching>. Experiments were carried out in parallel using a computing cluster; each experiment required less than a few hours with a standard CPU and less than 5GB of memory (20 GB of memory are needed for the analysis of the SARS-CoV-2 DNA data).

### Acknowledgements

M. S. is supported by NSF grant DMS 2210637 and by an Amazon Research Award. S. F. is also affiliated to IMATI-CNR “Enrico Magenes” (Milan, Italy), and received funding from the European Research Council under the European Union’s Horizon 2020 research and innovation programme

under grant No 817257. The authors are grateful to three anonymous reviewers for helpful comments and an insightful discussion.

## References

- [1] Jayadev Misra and David Gries. Finding repeated elements. *Science of computer programming*, 2(2):143–152, 1982.
- [2] Moses Charikar, Kevin Chen, and Martin Farach-Colton. Finding frequent items in data streams. In *International Colloquium on Automata, Languages, and Programming*, pages 693–703. Springer, 2002.
- [3] Qinfeng Shi, James Petterson, Gideon Dror, John Langford, Alex Smola, and SVN Vishwanathan. Hash kernels for structured data. *Journal of Machine Learning Research*, 10(11), 2009.
- [4] Stuart Schechter, Cormac Herley, and Michael Mitzenmacher. Popularity is everything: A new approach to protecting passwords from {Statistical-Guessing} attacks. In *5th USENIX Workshop on Hot Topics in Security (HotSec 10)*, 2010.
- [5] Amit Goyal, Hal Daumé III, and Graham Cormode. Sketch algorithms for estimating point queries in nlp. In *Proceedings of the 2012 joint conference on empirical methods in natural language processing and computational natural language learning*, pages 1093–1103, 2012.
- [6] Qingpeng Zhang, Jason Pell, Rosangela Canino-Koning, Adina Chuang Howe, and C Titus Brown. These are not the k-mers you are looking for: efficient online k-mer counting using a probabilistic data structure. *PLoS one*, 9(7):e101271, 2014.
- [7] Graham Cormode, Somesh Jha, Tejas Kulkarni, Ninghui Li, Divesh Srivastava, and Tianhao Wang. Privacy at scale: Local differential privacy in practice. In *Proceedings of the 2018 International Conference on Management of Data*, pages 1655–1658, 2018.
- [8] Can Kockan, Kaiyuan Zhu, Natnatee Dokmai, Nikolai Karpov, M Oguzhan Kulekci, David P Woodruff, and S Cenk Sahinalp. Sketching algorithms for genomic data analysis and querying in a secure enclave. *Nature methods*, 17(3):295–301, 2020.
- [9] Graham Cormode and Ke Yi. *Small summaries for big data*. Cambridge University Press, 2020.
- [10] Graham Cormode and Shan Muthukrishnan. An improved data stream summary: the count-min sketch and its applications. *Journal of Algorithms*, 55(1):58–75, 2005.
- [11] Daniel Ting. Count-min: Optimal estimation and tight error bounds using empirical error distributions. In *Proceedings of the 24th ACM SIGKDD International Conference on Knowledge Discovery & Data Mining*, pages 2319–2328, 2018.
- [12] Cristian Estan and George Varghese. New directions in traffic measurement and accounting. In *Proceedings of the 2002 conference on Applications, technologies, architectures, and protocols for computer communications*, pages 323–336, 2002.
- [13] Diana Cai, Michael Mitzenmacher, and Ryan P Adams. A Bayesian nonparametric view on count-min sketch. In *Advances in Neural Information Processing Systems 31*, pages 8782–8791, 2018.
- [14] Emanuele Dolera, Stefano Favaro, and Stefano Peluchetti. A Bayesian nonparametric approach to count-min sketch under power-law data streams. In *International Conference on Artificial Intelligence and Statistics*, pages 226–234. PMLR, 2021.
- [15] Vladimir Vovk, Alex Gammerman, and Glenn Shafer. *Algorithmic learning in a random world*. Springer, 2005.
- [16] Jing Lei, Max G’Sell, Alessandro Rinaldo, Ryan J. Tibshirani, and Larry Wasserman. Distribution-free predictive inference for regression. *Journal of the American Statistical Association*, 113(523):1094–1111, 2018.

- [17] Vladimir Vovk, Ilia Nouretdinov, and Alex Gammerman. On-line predictive linear regression. *Annals of Statistics*, 37(3):1566–1590, 2009.
- [18] Vladimir Vovk. Cross-conformal predictors. *Annals of Mathematics and Artificial Intelligence*, 74(1-2):9–28, 2015.
- [19] Jing Lei and Larry Wasserman. Distribution-free prediction bands for non-parametric regression. *Journal of the Royal Statistical Society: Series B (Statistical Methodology)*, 76(1):71–96, 2014.
- [20] Yaniv Romano, Evan Patterson, and Emmanuel Candès. Conformalized quantile regression. In *Advances in Neural Information Processing Systems*, pages 3538–3548, 2019.
- [21] Rafael Izbicki, Gilson T Shimizu, and Rafael B Stern. Flexible distribution-free conditional predictive bands using density estimators. *preprint at arXiv:1910.05575*, 2019.
- [22] Stephen Bates, Emmanuel Candès, Lihua Lei, Yaniv Romano, and Matteo Sesia. Testing for outliers with conformal p-values. *preprint at arXiv:2104.08279*, 2021.
- [23] Lihua Lei and Emmanuel Candès. Conformal inference of counterfactuals and individual treatment effects. *Journal of the Royal Statistical Society: Series B (Statistical Methodology)*.
- [24] Emmanuel Candès, Lihua Lei, and Zhimei Ren. Conformalized survival analysis. *arXiv preprint arXiv:2103.09763*, 2021.
- [25] Li Fan, Pei Cao, Jussara Almeida, and Andrei Z Broder. Summary cache: a scalable wide-area web cache sharing protocol. *IEEE/ACM transactions on networking*, 8(3):281–293, 2000.
- [26] Amit Goyal and Hal Daumé. Lossy conservative update (lcu) sketch: Succinct approximate count storage. In *Proceedings of the AAAI Conference on Artificial Intelligence*, volume 25, pages 878–883, 2011.
- [27] Guillaume Pitel and Geoffroy Fouquier. Count-min-log sketch: Approximately counting with approximate counters. *arXiv preprint arXiv:1502.04885*, 2015.
- [28] Chen-Yu Hsu, Piotr Indyk, Dina Katabi, and Ali Vakilian. Learning-based frequency estimation algorithms. In *International Conference on Learning Representations*, 2019.
- [29] Tanqiu Jiang, Yi Li, Honghao Lin, Yisong Ruan, and David P Woodruff. Learning-augmented data stream algorithms. In *International Conference on Learning Representations*, 2019.
- [30] Yaniv Romano, Matteo Sesia, and Emmanuel Candès. Classification with valid and adaptive coverage. *Advances in Neural Information Processing Systems*, 33:3581–3591, 2020.
- [31] Anastasios Angelopoulos, Stephen Bates, Jitendra Malik, and Michael I Jordan. Uncertainty sets for image classifiers using conformal prediction. *arXiv preprint arXiv:2009.14193*, 2020.
- [32] Chirag Gupta, Arun K Kuchibhotla, and Aaditya K Ramdas. Nested conformal prediction and quantile out-of-bag ensemble methods. *preprint at arXiv:1910.10562*, 2019.
- [33] Vladimir Vovk, David Lindsay, Ilia Nouretdinov, and Alex Gammerman. Mondrian confidence machine. Technical report, Royal Holloway, University of London, 2003.
- [34] Mauricio Sadinle, Jing Lei, and Larry Wasserman. Least ambiguous set-valued classifiers with bounded error levels. *Journal of the American Statistical Association*, 114(525):223–234, 2019.
- [35] Rina Foygel Barber, Emmanuel J Candès, Aaditya Ramdas, and Ryan J Tibshirani. The limits of distribution-free conditional predictive inference. *Information and Inference: A Journal of the IMA*, 10(2):455–482, 2021.
- [36] Victor Chernozhukov, Kaspar Wüthrich, and Yinchu Zhu. Distributional conformal prediction. *Proceedings of the National Academy of Sciences*, 118(48), 2021.

- [37] Matteo Sesia and Yaniv Romano. Conformal prediction using conditional histograms. *Advances in Neural Information Processing Systems*, 34, 2021.
- [38] James W. Taylor. A quantile regression neural network approach to estimating the conditional density of multiperiod returns. *Journal of Forecasting*, 19(4):299–311, 2000.
- [39] Nicolai Meinshausen. Quantile regression forests. *Journal of Machine Learning Research*, 7: 983–999, 2006.
- [40] Alexander Henzi, Johanna F. Ziegel, and Tilmann Gneiting. Isotonic distributional regression. *Journal of the Royal Statistical Society: Series B (Statistical Methodology)*, 83(5):963–993, 2021.
- [41] Jim Pitman and Marc Yor. The two parameter poisson-dirichlet distribution derived from a stable subordinator. *The Annals of Probability*, 25:855–900, 1997.
- [42] S. Thomas Ferguson. A Bayesian analysis of some nonparametric problems. *The Annals of Statistics*, 1:209–230, 1973.
- [43] Eneida L Hatcher, Sergey A Zhdanov, Yiming Bao, Olga Blinkova, Eric P Nawrocki, Yuri Ostapchuck, Alejandro A Schäffer, and J Rodney Brister. Virus variation resource–improved response to emergent viral outbreaks. *Nucleic acids research*, 45(D1):D482–D490, 2017.
- [44] Dhruv Medarametla and Emmanuel Candès. Distribution-free conditional median inference. *Electronic Journal of Statistics*, 15(2):4625–4658, 2021.
- [45] Steven Bird, Ewan Klein, and Edward Loper. *Natural language processing with Python: analyzing text with the natural language toolkit*. ” O’Reilly Media, Inc.”, 2009.
- [46] Project Gutenberg. Project Gutenberg. [www.gutenberg.org](http://www.gutenberg.org). Accessed: 2022-02-05.
- [47] Matteo Sesia and Emmanuel J Candès. A comparison of some conformal quantile regression methods. *Stat*, 9(1):e261, 2020.

## A1 Additional methodological details

### A1.1 The CMS algorithm

---

#### Algorithm A1 CMS

---

**Input:** Data set  $Z_1, \dots, Z_m$ . Sketch dimensions  $d, w$ . Hash functions  $h_1, \dots, h_d$ . Query  $z$ .

**Initialize:**  $C_{j,k} = 0$  for all  $j \in [d], k \in [w]$ .

**for**  $i = 1, \dots, m$  **do**

**for**  $j = 1, \dots, d$  **do**

**Increment**  $C_{j,h_j(Z_i)} \leftarrow C_{j,h_j(Z_i)} + 1$

**end for**

**end for**

**Compute**  $\hat{f}_{\text{up}}^{\text{CMS}}(z) = \min_{j \in [d]} \{C_{j,h_j(z)}\}$ .

**Output:** deterministic upper-bound for the frequency of  $z$  in the data set:  $\hat{f}_{\text{up}}^{\text{CMS}}(z)$ .

---

## A1.2 The CMS-CU algorithm

---

### Algorithm A2 CMS-CU

---

**Input:** Data set  $Z_1, \dots, Z_m$ . Sketch dimensions  $d, w$ . Hash functions  $h_1, \dots, h_d$ . Query  $z$ .  
**Initialize:**  $C_{j,k} = 0$  for all  $j \in [d], k \in [w]$ .  
**for**  $i = 1, \dots, m$  **do**  
    **Compute**  $j^* = \arg \min_{j \in [d]} C_{j, h_j(Z_i)}$ .  
    **Increment**  $C_{j^*, h_{j^*}(Z_i)} \leftarrow C_{j^*, h_{j^*}(Z_i)} + 1$   
**end for**  
**Compute**  $\hat{f}_{\text{up}}^{\text{CMS-CU}}(z) = \min_{j \in [d]} \{C_{j, h_j(z)}\}$ .  
**Output:** deterministic upper-bound for the frequency of  $z$  in the data set:  $\hat{f}_{\text{up}}^{\text{CMS-CU}}(z)$ .

---

## A1.3 Conformalized sketching

---

### Algorithm A3 Conformalized sketching

---

**Input:** Data set  $Z_1, \dots, Z_m$ . Sketching function  $\phi$ . Warm-up duration  $m_0 \ll m$ .  
A (trainable) rule for computing nested intervals  $[\hat{L}_{m,\alpha}(\cdot; t), \hat{U}_{m,\alpha}(\cdot; t)]$ ,  $t \in \mathcal{T}$ .  
Number of data points  $m_0^{\text{train}} < m_0$  used for training  $[\hat{L}_{m,\alpha}(\cdot; t), \hat{U}_{m,\alpha}(\cdot; t)]$ .  
A partition  $\mathcal{B} = (B_1, \dots, B_L)$  of  $\{0, \dots, m\}$  into  $L$  intervals.  
Random query  $Z_{m+1}$ . Desired coverage level  $1 - \alpha \in (0, 1)$ .  
**Initialize** a sparse dictionary  $f_{m_0}^{\text{wu}}(z) = 0, \forall z \in \mathcal{Z}$ .  
**for**  $i = 1, \dots, m_0$  **do**  
    **Increment**  $f_{m_0}^{\text{wu}}(Z_i) \leftarrow f_{m_0}^{\text{wu}}(Z_i) + 1$ .  
**end for**  
**Initialize** a sparse dictionary  $f_{m-m_0}^{\text{sv}}(z) = 0, \forall z \in \mathcal{Z}$ .  
**Initialize** an empty sketch  $\phi(\emptyset)$ .  
**for**  $i = m_0 + 1, \dots, m$  **do**  
    **Update** the sketch  $\phi$  with the new observation  $Z_i$ .  
    **if**  $f_{m_0}^{\text{wu}}(Z_i) > 0$  **then**  
        **Increment**  $f_{m-m_0}^{\text{sv}}(Z_i) \leftarrow f_{m-m_0}^{\text{sv}}(Z_i) + 1$ .  
    **end if**  
**end for**  
**Train**  $[\hat{L}_{m,\alpha}(\cdot; t), \hat{U}_{m,\alpha}(\cdot; t)]$  using the data in  $\{(X_i, Y_i)\}_{i=1}^{m_0^{\text{train}}}$ .  
**for**  $i = m_0^{\text{train}} + 1, \dots, m_0$  **do**  
    **Set**  $X_i = (Z_i, \phi(Z_{m_0+1}, \dots, Z_m))$  as in (12).  
    **Set**  $Y_i = f_{m-m_0}^{\text{sv}}(Z_i)$ .  
    **Compute** the conformity score  $E(X_i, Y_i)$  with (5), using  $[\hat{L}_{m,\alpha}(\cdot; t), \hat{U}_{m,\alpha}(\cdot; t)]$ .  
    **Assign** each score  $E(X_i, Y_i)$  to an appropriate frequency bin  $B \in \mathcal{B}$  based on  $Y_i$ .  
**end for**  
**for**  $l = 1, \dots, L$  **do**  
    **Compute**  $\hat{Q}_{n_l, 1-\alpha}(B_l)$  as the  $\lceil (1-\alpha)(n_l + 1) \rceil$  smallest value among the  $n_l$  scores in bin  $B_l$ .  
**end for**  
**Set**  $\hat{Q}_{n, 1-\alpha}^* = \max_l \hat{Q}_{n_l, 1-\alpha}(B_l)$ .  
**Set**  $X_{m+1} = (Z_{m+1}, \phi(Z_{m_0+1}, \dots, Z_m))$  as in (12).  
**Output:** a  $(1 - \alpha)$ -level confidence interval

$$\left[ f_{m_0}^{\text{wu}}(Z_{m+1}) + \hat{L}_{m,\alpha}(X_{m+1}; \hat{Q}_{n, 1-\alpha}^*), f_{m_0}^{\text{wu}}(Z_{m+1}) + \hat{U}_{m,\alpha}(X_{m+1}; \hat{Q}_{n, 1-\alpha}^*) \right]$$

for the unobserved frequency  $f_m(Z_{m+1})$  of  $Z_{m+1}$  defined in (2).

---

## A1.4 Constructing two-sided conformal confidence intervals

This section describes two alternative methods for constructing two-sided conformal confidence intervals. The first method, explained in Section A1.4.1, consists of directly calibrating a sequence

of nested two-sided intervals, as outlined in Section 3.3. The second method, explained in Section A1.4.2, consists of separately calibrating two sequences of lower and upper one-sided confidence intervals, each adopting the significance level  $\alpha/2$  instead of  $\alpha$ . The second approach is easier to implement compared to the first one, building upon the techniques detailed earlier in this paper, but it may be less statistically efficient.

#### A1.4.1 Construction based on conditional histograms

Two-sided conformal confidence intervals for  $f_m(X_{m+1})$  can be constructed by following the general recipe outlined in Section 3.3. To implement this method practically, one needs to fix an increasing sequence of candidate intervals  $[\hat{L}_{m,\alpha}(\cdot; t), \hat{U}_{m,\alpha}(\cdot; t)]$ , depending on  $Z_{m+1}$  and  $\phi(Z_{m_0+1}, \dots, Z_m)$ . Possible choices for such sequence may be directly borrowed from the existing literature on conformal inference for regression, including for example the quantile regression approach of [20] or the conditional histogram approach of [37]. Here, we describe a particular implementation that combines the idea in [37] with a Bayesian model, in continuity with the works of [13, 14] on Bayesian empirical frequency estimation from sketched data. However, the same idea could easily accommodate a quantile regression model or any other machine learning algorithm instead of the Bayesian model, as explained in [37]. Note that the following paragraphs largely retrace the same steps as in [37], which are however useful to recap here to make the presentation self contained.

For any  $j \in [m]$ , let  $\hat{\varphi}_j(x)$  indicate the posterior probability of  $f_m(X_{m+1}) = j$  for  $X_{m+1} = x$  as estimated by any Bayesian model for frequency estimation given sketched data, such as that of [13] based on a Dirichlet process prior, for example. For convenience of notation, we will sometimes refer to the full posterior distribution of  $f_m(X_{m+1})$  simply as  $\hat{\varphi}$ . Note that, in general, the form of the posterior distribution  $\hat{\varphi}$  may depend on  $m$  as well as on the sketched data in  $\phi(Z_{m_0+1}, \dots, Z_m)$ . Following in the footsteps of [37], define the following bi-valued function  $\mathcal{S}$  taking as input a query  $x$ , the posterior distribution  $\hat{\varphi}$ , a scalar threshold  $t \in [0, 1]$ , and two intervals  $S^-, S^+ \subseteq \{1, \dots, m\}$ :

$$\mathcal{S}(x, \hat{\varphi}, S^-, S^+, t) := \arg \min_{(l, u) \in \{1, \dots, m\}^2 : l \leq u} \left\{ |u - l| : \sum_{j=l}^u \hat{\varphi}_j(x) \geq t, S^- \subseteq [l, u] \subseteq S^+ \right\}. \quad (15)$$

Above, it is implied that we choose the value of  $(l, u)$  minimizing  $\sum_{j=l}^u \hat{\varphi}_j(x)$  among the feasible ones with minimal  $|u - l|$ , whenever the optimization problem does not have a unique solution. Therefore, we can assume without loss of generality that (15) has a unique solution; if that is not the case, we can break the ties at random by adding a little noise to  $\hat{\varphi}$ . As explained in [37], the problem defined in (15) can be solved efficiently, at computational cost linear in  $m$ . Note that we will sometimes refer to sub-intervals of  $[m]$  as either contiguous subsets of  $\{1, \dots, m\}$  (e.g.,  $S^-$ ) or as pairs of lower and upper endpoints (e.g.,  $[l, u]$ ).

If  $S^- = \emptyset$  and  $S^+ = \{1, \dots, m\}$ , the expression in (15) computes the shortest possible interval with total posterior probability mass above  $t$ . In general, the optimization in (15) involves the additional *nesting* constraint that the output  $\mathcal{S}$  must satisfy  $S^- \subseteq \mathcal{S} \subseteq S^+$ , which will be needed to guarantee the resulting sequence of confidence intervals indexed by  $t$  is nested. Note that the inequality in (15) involving  $t$  may not be binding at the optimal solution due to the discrete nature of the optimization problem. However, the above construction could be easily modified by introducing some suitable randomization leading to confidence intervals that are even tighter on average, as explained in [37].

For any integer  $T \geq 1$ , consider an increasing sequence  $t_\tau \in [0, 1]$ , for  $\tau \in \{0, \dots, T\}$ . A nested sequence of  $T$  intervals indexed by  $\tau \in \{0, \dots, T\}$ , which may be written in the form of

$$S_t = [\hat{L}_{m,\alpha}(X_{m+1}; t_\tau), \hat{U}_{m,\alpha}(X_{m+1}; t_\tau)],$$

for appropriate lower and upper endpoints  $\hat{L}_{m,\alpha}(X_{m+1}; t_\tau)$  and  $\hat{U}_{m,\alpha}(X_{m+1}; t_\tau)$ , respectively, is then constructed from (15) as follows. First, fix any *starting index*  $\bar{\tau} \in \{0, 1, \dots, T\}$  and define  $S_{\bar{\tau}}$  by applying (15) without the nesting constraints (with  $S^- = \emptyset$  and  $S^+ = \{1, \dots, m\}$ ):

$$S_{\bar{\tau}} := \mathcal{S}(x, \hat{\varphi}, \emptyset, \{1, \dots, m\}, t_{\bar{\tau}}), \quad (16)$$

Note the explicit dependence on  $x$  and  $\hat{\varphi}$  of the left-hand-side above is omitted for simplicity, although it is important to keep in mind that  $S_{\bar{\tau}}$  does of course depend on these quantities.

Having computed the initial interval  $S_{\bar{\tau}}$ , we recursively extend the definition to the wider intervals indexed by  $\tau = \bar{\tau} + 1, \dots, T$  as follows:

$$S_{\tau} := \mathcal{S}(x, \hat{\varphi}, S_{\tau-1}, \{1, \dots, m\}, t_{\tau}).$$

See [37] for a schematic visualization of this step. Similarly, the narrower intervals  $S_{\tau}$  indexed by  $\tau = \bar{\tau} - 1, \bar{\tau} - 2, \dots, 0$  are defined recursively as:

$$S_{\tau} := \mathcal{S}(x, \hat{\varphi}, \emptyset, S_{\tau+1}, t_{\tau}).$$

See [37] for a schematic visualization of this step. As a result of this construction, the sequence of intervals  $\{S_{\tau}\}_{\tau=0}^T$  is nested regardless of the starting point  $\bar{\tau}$  in (16), for which a typical choice is such that  $t_{\bar{\tau}} = 1 - \alpha$ . Then, two-sided conformal confidence intervals for  $f_m(X_{m+1})$  can be obtained by applying Algorithm A3 with this particular sequence of input nested intervals. We refer to [37] for further details on the construction of nested intervals outlined above.

#### A1.4.2 Construction based on a pair of one-sided intervals with Bonferroni correction

An alternative, and somewhat simpler, approach to building two-sided conformal confidence intervals for  $f_m(X_{m+1})$  at level  $1 - \alpha$  consists of constructing a pair of lower and upper one-sided confidence intervals at level  $1 - \alpha/2$ . In particular, consider the following two nested sequences  $S_t^l$  and  $S_t^u$  of one-sided confidence intervals, each indexed by a scalar parameter  $t$ :

$$S_t^l = [\hat{L}_{m,\alpha/2}(X_{m+1}; t), \hat{f}_{\text{up}}^{\text{CMS}}(X_{m+1})], \quad S_t^u = [0, \hat{U}_{m,\alpha/2}(X_{m+1}; t)],$$

where  $\hat{f}_{\text{up}}^{\text{CMS}}(X_{m+1})$  is a deterministic upper bound for the unknown true empirical frequency of  $X_{m+1}$ ; e.g., see Section 1.2. The sequences  $S_t^l$  and  $S_t^u$  can be separately calibrated using the conformal inference method described in Sections 3.3 and 3.4, for any given choice of frequency-range partition  $\mathcal{B}$ , as we shall make more precise below. This gives two distinct data-adaptive thresholds  $\hat{Q}_{n,1-\alpha/2}^{*,l}$  and  $\hat{Q}_{n,1-\alpha/2}^{*,u}$ , respectively, such that,  $\forall B \in \mathcal{B}$ ,

$$\mathbb{P} \left[ f_m(X_{m+1}) \geq \hat{L}_{m,\alpha/2}(X_{m+1}; \hat{Q}_{n,1-\alpha/2}^{*,l}) \mid f_m(Z_{m+1}) \in B \right] \geq 1 - \frac{\alpha}{2},$$

and

$$\mathbb{P} \left[ f_m(X_{m+1}) \leq \hat{U}_{m,\alpha/2}(X_{m+1}; \hat{Q}_{n,1-\alpha/2}^{*,u}) \mid f_m(Z_{m+1}) \in B \right] \geq 1 - \frac{\alpha}{2}.$$

By a union bound, we obtain that the following two-sided conformal confidence interval has valid coverage, in the sense of (8), at level  $1 - \alpha$ :

$$[\hat{L}_{m,\alpha/2}(X_{m+1}; \hat{Q}_{n,1-\alpha/2}^{*,l}), \hat{U}_{m,\alpha/2}(X_{m+1}; \hat{Q}_{n,1-\alpha/2}^{*,u})].$$

Different practical implementations are available to construct the sequences of candidate lower bounds  $\hat{L}_{m,\alpha/2}(X_{m+1}; t)$  and upper bounds  $\hat{U}_{m,\alpha/2}(X_{m+1}; t)$ . Two concrete examples are explained below.

**Constant conformity scores.** A simple option to construct the sequence  $\hat{L}_{m,\alpha/2}(X_{m+1}; t)$  is to directly apply the method described in Section 3.4, for example by shifting  $\hat{f}_{\text{up}}^{\text{CMS}}(X_{m+1})$  downward by a constant  $t$ . Then, the conformalized threshold  $\hat{Q}_{n,1-\alpha/2}^{*,l}$  can be calibrated exactly as described in Section 3.3. The sequence of candidate upper bounds  $\hat{U}_{m,\alpha/2}(X_{m+1}; t)$  can also be constructed similarly to  $\hat{L}_{m,\alpha/2}(X_{m+1}; t)$ , for example by adding a constant  $t$  to the trivial lower bound of 0, up to the deterministic upper bound  $\hat{f}_{\text{up}}^{\text{CMS}}(X_{m+1})$ . The threshold  $\hat{Q}_{n,1-\alpha/2}^{*,u}$  for  $\hat{U}_{m,\alpha/2}(X_{m+1}; t)$  can then be calibrated as usual with Algorithm A3.

**Bootstrap conformity scores.** An alternative option to construct the sequence  $\hat{L}_{m,\alpha/2}(X_{m+1}; t)$  consists of shifting downward by a constant  $t$  the bootstrap lower bound calculated with the method of [11], at level  $\alpha/2$ . Similarly, the sequence  $\hat{U}_{m,\alpha/2}(X_{m+1}; t)$  can be obtained by shifting upward by a constant  $t$  the analogous bootstrap upper bound at level  $1 - \alpha/2$ . Thus, in the special case of the vanilla CMS, our conformal confidence intervals based on these scores intuitively become very similar to the bootstrap confidence intervals of [11]. In general, however, the difference remains that the intervals of [11] rely on the linearity of the CMS, while ours are theoretically valid regardless of how the data are sketched. We have observed this option works well in practice, at least within the scope of our numerical experiments. Therefore, this is the implementation adopted in our numerical experiments described in Section A4.



## A1.5 Sampling from a Pitman-Yor predictive distribution

The data points are sampled sequentially from the following predictive distribution, which has parameters  $\lambda > 0$  and  $\sigma \in [0, 1)$ . After sampling  $Z_1$  from a standard normal distribution,  $\mathcal{N}(0, 1)$ , fix any  $i \geq 1$  and let  $Z_1, \dots, Z_i$  indicate the data stream observed up to that point. Denote by  $k_i$  the number of distinct elements within it, and by  $V_i = (V_{i,1}, \dots, V_{i,k_i})$  the set of such distinct values. Further, let  $c_{i,l}$  indicate the number of times that object  $V_{i,l}$  has been observed in  $Z_1, \dots, Z_i$ , for  $l \in \{1, \dots, k_i\}$ . Then,  $Z_{i+1}$  is generated as follows:

$$Z_{i+1} \mid Z_1, \dots, Z_i = \begin{cases} V_{i,l}, & \text{with probability } \frac{c_{i,l} - \sigma}{\lambda + i}, \text{ for } l \in \{1, \dots, k_i\}, \\ \mathcal{N}(0, 1), & \text{with probability } \frac{\lambda + k_i \sigma}{\lambda + i}. \end{cases}$$

Above, the second case which occurs with probability  $(\lambda + k_i \sigma)/(\lambda + i)$  corresponds to sampling a new unique value from the standard normal distribution.

## A2 Mathematical proofs

### A2.1 Proof of Proposition 1

*Proof.* Consider  $((X_{\pi(1)}, Y_{\pi(1)}), \dots, (X_{\pi(m_0)}, Y_{\pi(m_0)}), (X_{\pi(m+1)}, Y_{\pi(m+1)}))$  for any permutation  $\pi$  of  $\{1, \dots, m_0, m+1\}$ . This is equal to  $((X'_1, Y'_1), \dots, (X'_{m_0}, Y'_{m_0}), (X'_{m+1}, Y'_{m+1}))$ , defined by applying the functions in (11)–(12) to a shuffled data set  $Z_{\tilde{\pi}(1)}, \dots, Z_{\tilde{\pi}(m+1)}$ , where  $\tilde{\pi}$  indicates a permutation of  $\{1, \dots, m+1\}$  that agrees with  $\pi$  on  $\{1, \dots, m_0, m+1\}$  and leaves  $\{m_0+1, \dots, m\}$  unchanged. Therefore,

$$\begin{aligned} & ((X_{\pi(1)}, Y_{\pi(1)}), \dots, (X_{\pi(m_0)}, Y_{\pi(m_0)}), (X_{\pi(m+1)}, Y_{\pi(m+1)})) \\ &= ((X'_1, Y'_1), \dots, (X'_{m_0}, Y'_{m_0}), (X'_{m+1}, Y'_{m+1})) \\ &\stackrel{d}{=} ((X_1, Y_1), \dots, (X_{m_0}, Y_{m_0}), (X_{m+1}, Y_{m+1})), \end{aligned}$$

where the last equality in distribution follows directly from the assumption that  $Z_1, \dots, Z_{m+1}$  are exchangeable.  $\square$

### A2.2 Proof of Theorem 2

*Proof.* The following notation will be helpful: let  $B(Y_i) \in \mathcal{B}$  indicate the frequency bin into which  $Y_i$  belongs, for  $i \in \{1, \dots, m_0, m+1\}$ . We begin by proving the result for the simpler case in which Algorithm A3 is applied using conformity scores that do not require training, in which case  $m_0^{\text{train}} = 0$ . For  $i \in \{1, \dots, m_0, m+1\}$ , define the random variables  $Y_i$  and  $X_i$  as in (11)–(12), respectively. We already know from Proposition 1 that  $(X_1, Y_1), \dots, (X_{m_0}, Y_{m_0}), (X_{m+1}, Y_{m+1})$  are exchangeable. This implies that the conformity scores  $E(X_i, Y_i)$  are exchangeable with one another, for  $i \in \{1, \dots, m_0, m+1\}$ , because each of them only depends on  $X_i, Y_i$  and on the separate data points in the sketch  $\phi(Z_{m_0+1}, \dots, Z_m)$ . Therefore,  $E_{m+1}$  is also exchangeable with the subset of conformity scores with indices in  $\{i \in \{1, \dots, m_0\} : B(Y_i) = B(Y_{m+1})\}$ . Now, fix any bin  $B^* \in \mathcal{B}$  and assume  $B(Y_{m+1}) = B^*$ . Now, note that the interval output by Algorithm A3 does not cover the true frequency  $f_m(Z_{m+1})$  if and only if  $E_{m+1} > \hat{Q}_{n,1-\alpha} \geq \hat{Q}_{n_i,1-\alpha}(B^*)$ . However, a standard exchangeability argument for the conformity scores in  $\{i \in \{1, \dots, m_0\} : B(Y_i) = B^*\}$  shows that  $\mathbb{P}[E_{m+1} > \hat{Q}_{n_i,1-\alpha}(B^*) \mid B(Y_{m+1}) = B^*] \leq 1 - \alpha$ ; for example, see Lemma 1 of [20]. This completes the first part of the proof. The second part with  $m_0^{\text{train}} > 0$  follows very similarly: Proposition 1 implies that  $(X_{m_0^{\text{train}}+1}, Y_{m_0^{\text{train}}+1}), \dots, (X_{m_0}, Y_{m_0}), (X_{m+1}, Y_{m+1})$  are exchangeable, and so must be the conformity scores  $E_i$  for  $i \in \{m_0^{\text{train}}+1, \dots, m_0, m+1\}$  because each of them only depends on the corresponding  $X_i, Y_i$  and on the separate set of observations indexed by  $\{1, \dots, m_0^{\text{train}}\}$ , as well as on the sketch  $\phi(Z_{m_0+1}, \dots, Z_m)$ . The rest of the proof is exactly the same as in the first part because the empirical quantiles  $\hat{Q}_{n_i,1-\alpha}(B)$  are only computed on subsets of the data indexed by  $\{m_0^{\text{train}}+1, \dots, m_0\}$ .  $\square$

### A3 Supplementary figures and tables

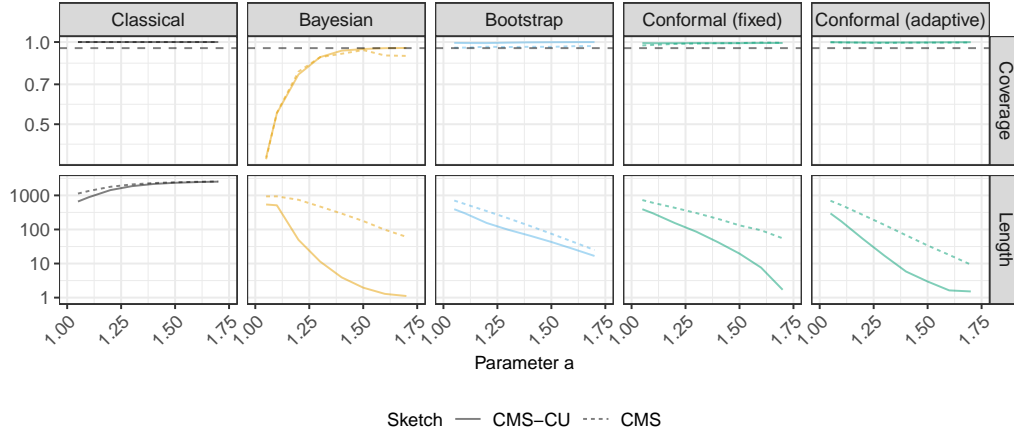


Figure A1: Performance of 95% confidence intervals for random frequency queries, based on synthetic data from a Zipf distribution. The data are sketched with either the vanilla CMS or the CMS-CU. The results are shown as a function of the Zipf tail parameter  $a$ . Other details are as in Figure 1.

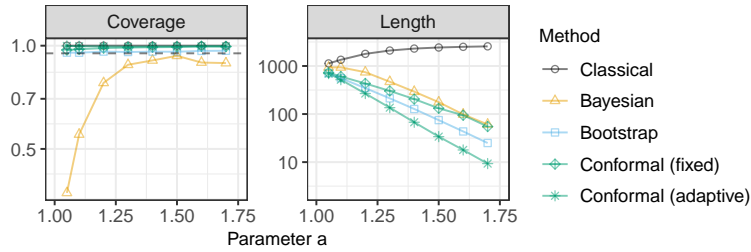


Figure A2: Performance of 95% confidence intervals for random frequency queries, based on synthetic data from a Zipf distribution, sketched with the vanilla CMS. The results are shown as a function of the Zipf tail parameter  $a$ . Other details are as in Figure 1.

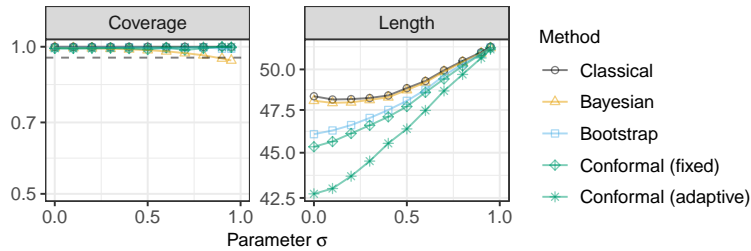


Figure A3: Empirical coverage and length of 95% confidence intervals for random frequency queries on a synthetic data set sampled from the predictive distribution of a Pitman-Yor process. The data are sketched with the CMS-CU. The results are shown as a function of the Pitman-Yor process parameter  $\sigma$ . Other details are as in Figure 1.

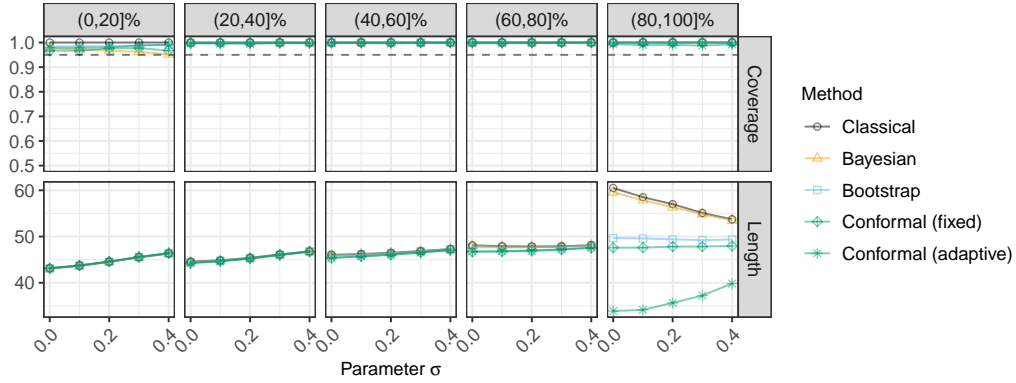


Figure A4: Performance of 95% confidence intervals for random frequency queries on a synthetic data set sampled from the predictive distribution of a Pitman-Yor process. The results are stratified by the quintile of the true query frequency. Other details are as in Figure A3.

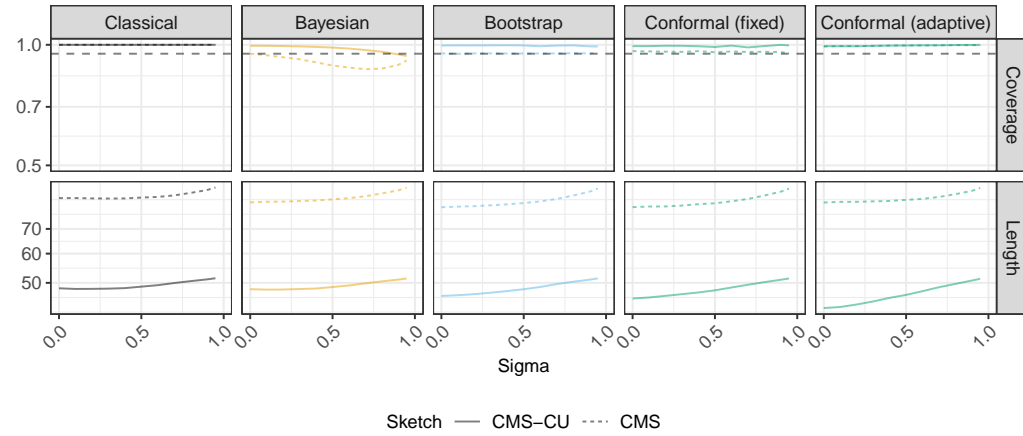


Figure A5: Performance of 95% confidence intervals for random frequency queries, based on synthetic data sampled from the predictive distribution of a Pitman-Yor process and sketched with either the vanilla CMS or the CMS-CU. The results are shown as a function of the Pitman-Yor process parameter  $\sigma$ . Other details are as in Figure A3.

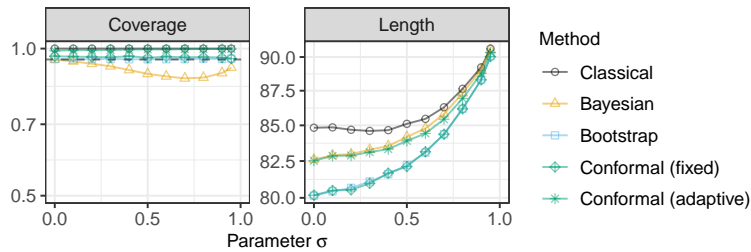


Figure A6: Performance of 95% confidence intervals for random frequency queries, based on synthetic data sampled from the predictive distribution of a Pitman-Yor process and sketched with the vanilla CMS. The results are shown as a function of the Pitman-Yor process parameter  $\sigma$ . Other details are as in Figure A3.

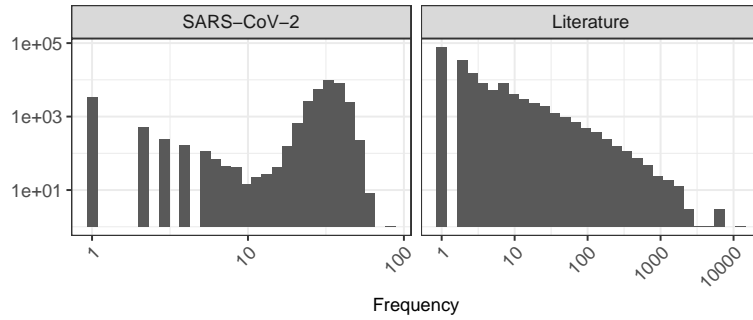


Figure A7: True frequency distribution of unique objects in two real data sets. Left: sequenced SARS-CoV-2 DNA 16-mers. Right: English 2-grams in a corpus of classic English literature.

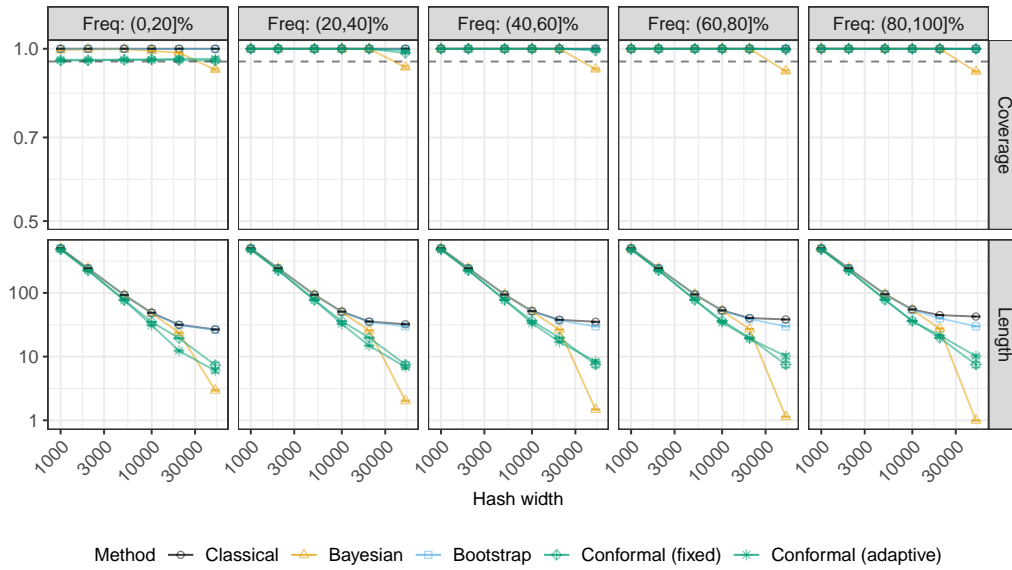


Figure A8: Performance of 95% confidence intervals for random frequency queries on SARS-CoV-2 sequence data sketched with the CMS-CU. The results are shown as a function of the hash width and stratified by the quintile of the true query frequency. Other details are as in Figure 3.

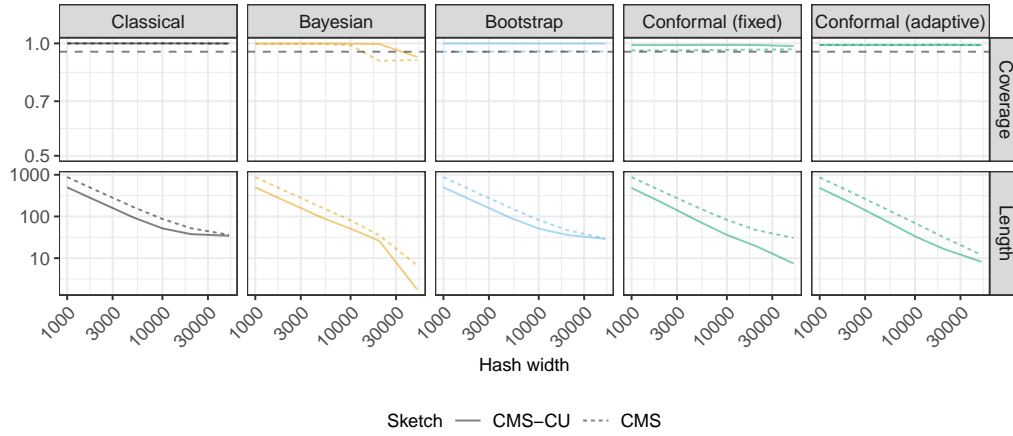


Figure A9: Performance of 95% confidence intervals for random frequency queries on SARS-CoV-2 sequence data. The data are sketched with either the vanilla CMS or the CMS-CU. The results are shown as a function of the hash width. Other details are as in Figure 3.

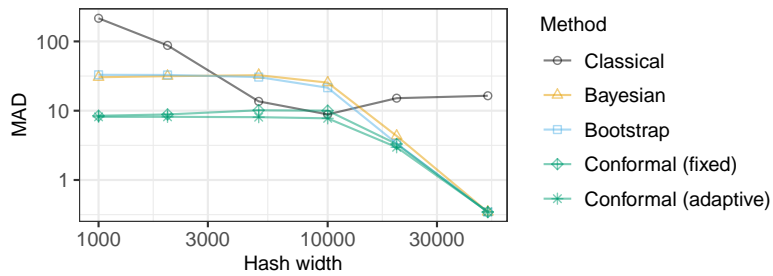


Figure A10: Median absolute deviation of point estimates for random frequency queries on SARS-CoV-2 sequence data sketched with the CMS-CU. The results are shown as a function of the hash width. Other details are as in Figure 3.

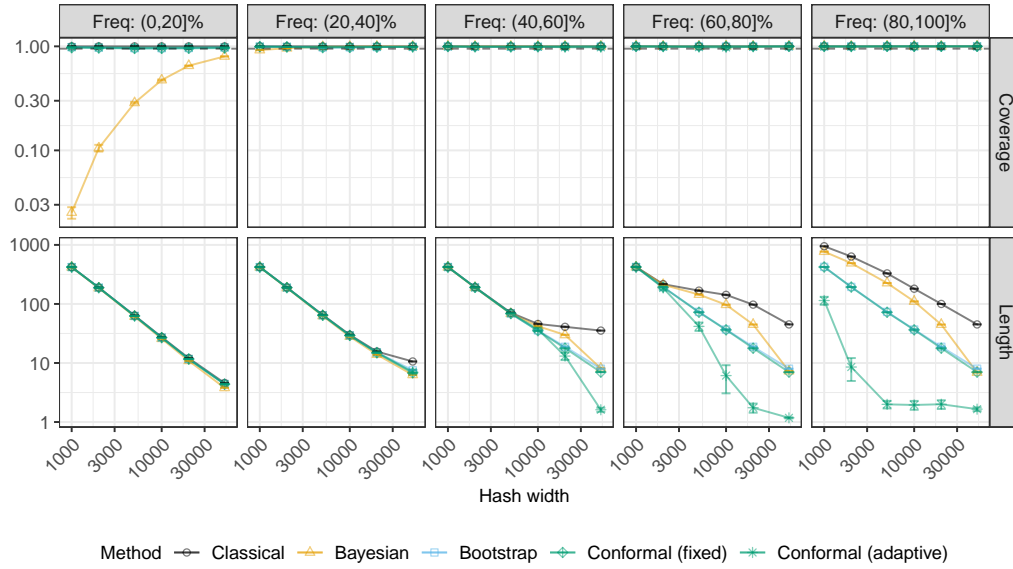


Figure A11: Performance of 95% confidence intervals for random frequency queries on a data set of 2-grams in classic English literature, sketched with the CMS-CU. The results are shown as a function of the hash width and stratified by the quintile of the true query frequency. Other details are as in Figure 4.

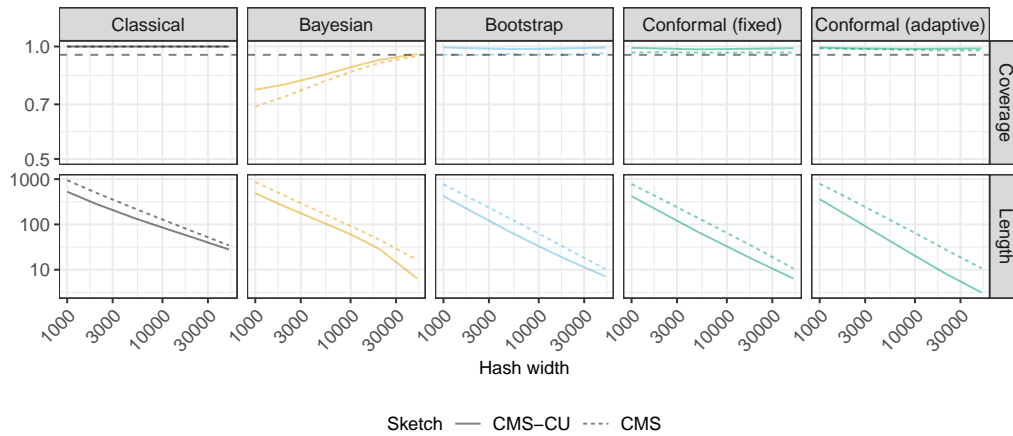


Figure A12: Performance of 95% confidence intervals for random frequency queries on a data set of 2-grams in classic English literature. The data are sketched with either the vanilla CMS or the CMS-CU. The results are shown as a function of the hash width. Other details are as in Figure 4.

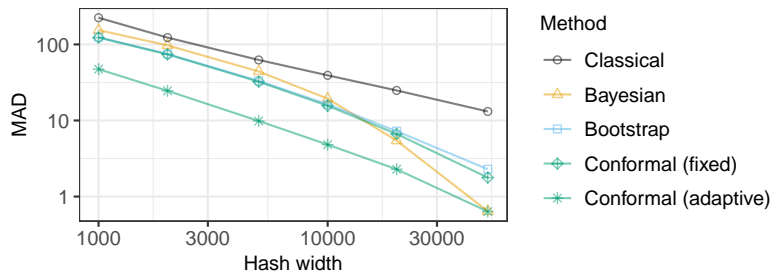


Figure A13: Median absolute deviation of point estimates for random frequency queries on a data set of 2-grams in classic English literature, sketched with the CMS-CU. The results are shown as a function of the hash width. Other details are as in Figure 4.

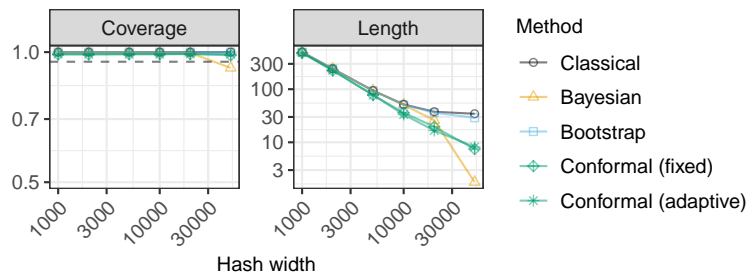


Figure A14: Performance of 95% confidence intervals for random frequency queries, on a sketched data set of 2-grams in classic English literature, keeping only unique queries. The coverage is defined as the empirical proportion of unique queries whose frequency is correctly covered by the output confidence intervals. The data are sketched with the CMS-CU. The results are shown as a function of the hash width. Other details are as in Figure 3.

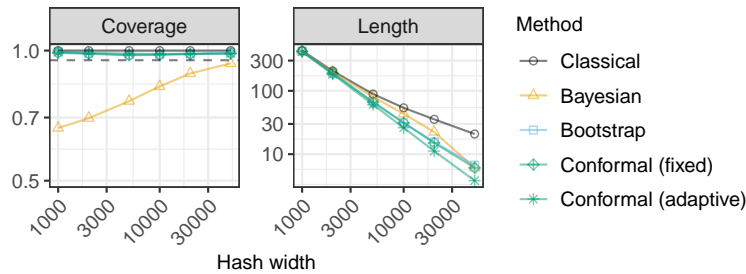


Figure A15: Performance of 95% confidence intervals for random frequency queries, on a sketched data set of 2-grams in classic English literature, keeping only unique queries. The coverage is defined as the empirical proportion of unique queries whose frequency is correctly covered by the output confidence intervals. The results are shown as a function of the hash width. Other details are as in Figure 4.

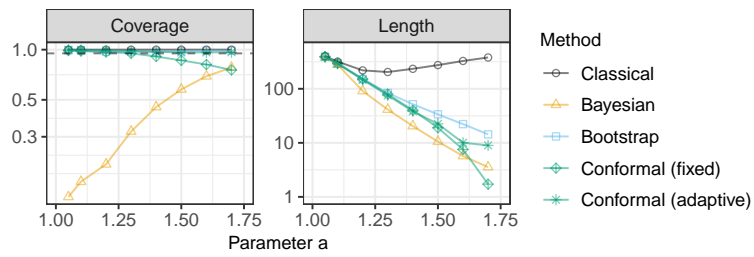


Figure A16: Performance of confidence intervals for random frequency queries, keeping only unique queries. The coverage is defined as the empirical proportion of unique queries whose frequency is correctly covered by the output confidence intervals. The results are shown as a function of the Zipf tail parameter  $a$ . Other details are as in Figure 1.



Table A1: True frequencies, deterministic upper bounds, and 95% lower bounds for some a few random queries in two sketched data sets. Sketching with CMS-CU with  $w = 50,000$ . Lower bounds written in green are below the true frequency; those in red are above. For each query, the highest lowest bound below the true frequency is highlighted in bold.

Data	Frequency	Upper bound	95% Lower bound				
			Classical	Bayesian	Bootstrap	Conformal	
						Fixed	Adaptive
<b>SARS-CoV-2</b>							
AATTATTATAAGAAAG	81	81	26	<b>81</b>	52	50	36
TCAGACAACTACTATT	76	76	21	<b>55</b>	47	45	32
AAAGTTGATGGTGTG	73	73	18	<b>59</b>	44	42	31
CAATTATTATAAGAAA	63	63	8	<b>48</b>	34	32	26
ATCAGACAACTACTAT	60	60	5	<b>44</b>	31	29	26
ACCTTTGACAATCTTA	55	55	0	<b>52</b>	26	24	27
ATTTGAAGTCACCTAA	55	55	0	<b>55</b>	26	24	27
CATGCAAATTACATAT	54	54	0	<b>54</b>	25	23	26
GAATTTACAGTATTC	54	54	0	<b>54</b>	25	23	27
TTTGTAGAAAACCCAG	53	53	0	<b>53</b>	24	22	27
AGTTGCAGAGTGGTTT	24	24	0	13	0	0	<b>20</b>
TCTTCACAATTGGAAC	24	24	0	12	0	1	<b>20</b>
TTCTGCTCGCATAGTG	24	24	0	12	0	0	<b>20</b>
CTACTTTAGATTCGAA	23	23	0	11	0	0	<b>19</b>
GCTGGTGTCTCTATCT	23	23	0	<b>23</b>	0	1	19
TTCTAAGAAGCCTCGG	23	24	0	14	0	0	<b>20</b>
GGGCTGTTGTTCTTGT	22	24	0	12	0	0	<b>20</b>
ACGTTTCGTGTTGTTTT	20	20	0	<b>20</b>	0	0	16
GAAGTCTTTGAATGTG	20	20	0	<b>20</b>	0	0	16
CAAACCTGGTAATTTTT	3	3	0	<b>3</b>	0	0	0
<b>Literature</b>							
of the	12565	12568	12513	12544	12557	12556	<b>12562</b>
in the	6188	6190	6135	6169	6179	6179	<b>6180</b>
and the	6173	6175	6120	6151	6164	6164	<b>6165</b>
the of	6015	6017	5962	5990	6006	6006	<b>6007</b>
the lord	4186	4195	4140	4165	4184	4184	4184
to the	3465	3467	3412	3445	3456	3456	<b>3463</b>
the and	2250	2251	2196	2227	2240	2240	<b>2248</b>
all the	2226	2230	2175	2207	2219	2219	<b>2224</b>
and he	2169	2173	2118	2153	2162	2162	<b>2167</b>
to be	2062	2064	2009	2043	2053	2053	<b>2060</b>
man on	22	29	0	10	18	18	18
their hand	22	24	0	9	13	13	0
no need	20	28	0	9	17	17	16
and brother	12	14	0	2	3	3	0
miss would	10	13	0	<b>3</b>	2	2	0
i please	8	12	0	<b>3</b>	1	1	1
also how	3	13	0	2	2	2	0
in under	3	9	0	<b>2</b>	0	0	0
ten old	3	6	0	<b>1</b>	0	0	0
fault he	1	9	0	<b>1</b>	0	0	0

Table A2: True frequencies, upper and lower bounds for a few random queries in two sketched data sets. Hash width  $w = 50,000$ . Other details are as in Table A1.

Data	Frequency	Upper bound	95% Lower bound				
			Classical	Bayesian	Bootstrap	Conformal	
						Fixed	Adaptive
<b>SARS-CoV-2</b>							
AATTATTATAAGAAAG	81	209	0	4	0	0	<b>18</b>
TCAGACAACTACTATT	76	213	0	8	0	0	<b>18</b>
AAAGTTGATGGTGTTG	73	130	0	2	0	1	<b>18</b>
CAATTATTATAAGAAA	63	233	0	4	11	6	<b>19</b>
ATCAGACAACTACTAT	60	179	0	2	0	0	<b>18</b>
ACCTTTGACAATCTTA	55	292	0	15	<b>70</b>	<b>67</b>	<b>22</b>
ATTTGAAGTCACCTAA	55	258	0	11	<b>36</b>	31	20
CATGCAAATTACATAT	54	204	0	3	0	0	<b>18</b>
GAATTTACAGTATTC	54	260	0	12	<b>38</b>	35	22
TTTGTAGAAAACCCAG	53	246	0	7	<b>24</b>	18	20
ATGCTGCAATCGTGCT	24	139	0	2	0	0	<b>17</b>
ATTTCTAATATTACA	24	92	0	1	0	0	<b>17</b>
CTCTATCATTATGGT	24	121	0	1	0	0	<b>17</b>
TGTTTTATTCTCTACA	24	199	0	3	0	1	<b>19</b>
CAGTACATCGATATCG	23	119	0	2	0	0	<b>17</b>
TAATGGTGACTTTTTG	23	92	0	1	0	0	<b>17</b>
CAACCATAAAAACCGT	22	105	0	1	0	0	<b>17</b>
AGTTATTTGACTCCTG	21	97	0	1	0	1	<b>18</b>
ATAAAGGAGTTGCACC	19	218	0	5	0	0	<b>18</b>
<b>Literature</b>							
of the	12565	12630	12086	12325	12463	12454	<b>12563</b>
in the	6188	6242	5698	5906	6075	6067	<b>6096</b>
and the	6173	6314	5770	5972	6147	6139	<b>6169</b>
the of	6015	6162	5618	5834	5995	5985	<b>6014</b>
the lord	4186	4289	3745	3975	4122	4114	<b>4185</b>
to the	3465	3558	3014	3217	3391	3380	<b>3464</b>
the and	2250	2413	1869	2081	2246	2237	<b>2249</b>
all the	2226	2346	1802	1993	2179	2170	<b>2225</b>
and he	2169	2293	1749	1937	2126	2117	<b>2168</b>
to be	2062	2121	1577	1770	1954	1945	<b>2061</b>
very for	15	59	0	2	0	0	0
and faithful	14	94	0	3	0	0	0
but found	9	74	0	2	0	0	0
my speech	6	98	0	3	0	0	0
of eight	5	66	0	2	0	0	0
and soul	4	140	0	6	0	0	0
her prow	3	79	0	2	0	0	0
usual as	2	56	0	2	0	0	0
a invitation	1	80	0	2	0	0	0
angular log	0	146	0	5	0	0	0

## A4 Additional experiments with two-sided confidence intervals

This section describes additional numerical experiments with synthetic data similar to those described in Figures 1 and A3, constructing two-sided instead of one-sided confidence intervals. For simplicity, we focus on one-sided 95% conformalized bootstrap confidence intervals based on the simpler Bonferroni approach described in Section A1.4.2. The performance of these intervals are compared to those of one and two-sided standard bootstrap confidence intervals obtained with the method of [11].

Figure A17 reports on results based on data generated from a Zipf distribution and sketched with the CMS-CU, similarly to Figure 1. Here, all methods achieve the desired 95% marginal coverage level, but the conformal confidence intervals are shorter when the Zipf tail parameter  $a$  is larger and hash collisions become rarer, consistently with Figure 1. It is interesting to note that the two-sided conformal confidence intervals are much narrower than their one-sided counterparts when  $a$  is small and hash collisions are very common, but this is not true if  $a$  is large. The latter is likely a limitation of the specific construction we have adopted, described in Section A1.4.2, which may be too conservative in some cases due to the Bonferroni correction. A suitable implementation of the more sophisticated conditional histogram [37] approach described in Section A1.4.1 should be expected to produce two-sided intervals that are always narrower than their one-sided counterparts. Figure A18 reports on results similar to those in Figure A17, with the only difference that now the data are sketched with the vanilla CMS instead of the CMS-CU.

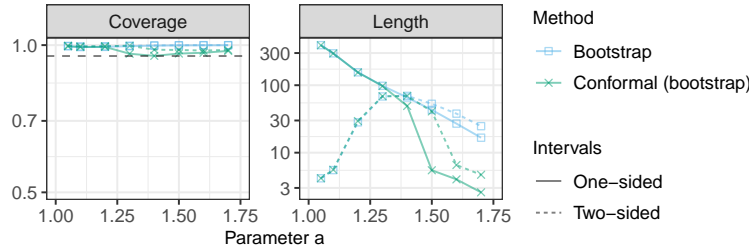


Figure A17: Performance of 95% one-sided and two-sided confidence intervals with data from a Zipf distribution, sketched with the CMS-CU. The results are shown as a function of the Zipf tail parameter  $a$ . Standard errors would be too small to be clearly visible in this figure, and are hence omitted. The two dashed curves for the two-sided intervals are nearly indistinguishable from one another for  $a < 1.3$ . Other details are as in Figure 1.

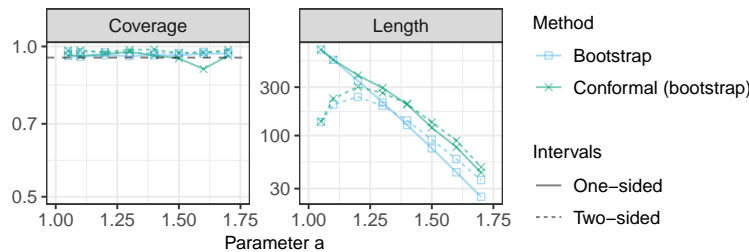


Figure A18: Performance of 95% one-sided and two-sided confidence intervals with data from a Zipf distribution, sketched with the vanilla CMS. The results are shown as a function of the Zipf tail parameter  $a$ . The two dashed curves for the two-sided intervals are nearly indistinguishable from one another for  $a < 1.1$ . Other details are as in Figure A17.

Figure A19 reports on results based on data generated from a Pitman-Yor process prior and sketched with the CMS-CU, similarly to Figure A3. As expected, the conformal confidence intervals are narrower than the bootstrap ones. Further, two-sided confidence intervals are much more efficient (narrower) compared to their one-sided counterparts, especially if the Pitman-Yor parameter  $\sigma$  is large and the number of hash collisions is high. Figure A20 reports on analogous results obtained with data sketched through the vanilla CMS instead of the CMS-CU.

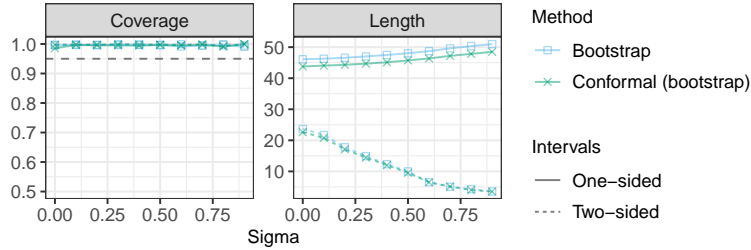


Figure A19: Performance of 95% one-sided and two-sided confidence intervals with data set sampled from the predictive distribution of a Pitman-Yor process and sketched with the CMS-CU. The results are shown as a function of the Pitman-Yor process parameter  $\sigma$ . The two dashed curves for the two-sided intervals are nearly indistinguishable from one another. Other details are as in Figure A3.

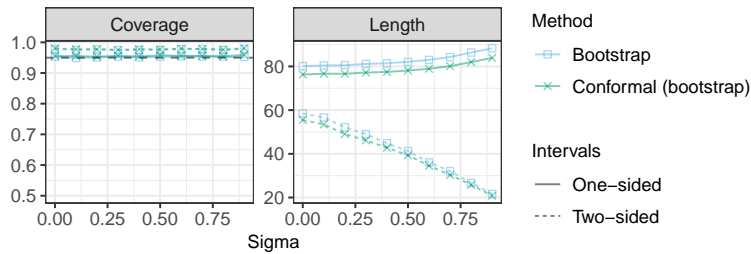


Figure A20: Performance of 95% one-sided and two-sided confidence intervals with data set sampled from the predictive distribution of a Pitman-Yor process and sketched with the vanilla CMS. The results are shown as a function of the Pitman-Yor process parameter  $\sigma$ . Other details are as in Figure A19.